

## AN EXPERIMENTAL INVESTIGATION OF LIQUID METAL MHPs

Except where reference is made to the work of others, the work described in this thesis is my own or was done in collaboration of my advisory committee.  
This thesis does not include proprietary or classified information.

---

Ashish Yudhishtir Palkar

Certificate of Approval:

---

Thomas Burch  
Visiting Assistant Professor  
Mechanical Engineering

---

Daniel K. Harris, Chair  
Associate Professor  
Mechanical Engineering

---

Robert Dean  
Assistant Professor  
Electrical and Computer Engineering

---

George T. Flowers  
Interim Dean  
Graduate School

AN EXPERIMENTAL INVESTIGATION OF LIQUID METAL MHPs

Ashish Yudhishtir Palkar

A Thesis

Submitted to

the Graduate Faculty of

Auburn University

in Partial Fulfillment of the

Requirements for the

Degree of

Master of Science

Auburn, Alabama  
December 17, 2007

AN EXPERIMENTAL INVESTIGATION OF LIQUID METAL MHPs

Ashish Yudhishtir Palkar

Permission is granted to Auburn University to make copies of this thesis at its discretion,  
upon request of individuals or institutions and at their expense.  
The author reserves all publication rights.

---

Signature of Author

---

Date of Graduation

## VITA

Ashish Yudhishtir Palkar, son of Yudhishtir V Palkar and Neela Y Palkar, was born on March 25<sup>th</sup> 1983 in Sangli, Maharashtra, India. In October 2000, he entered the PVG's College of Engineering and Technology at University of Pune, Maharashtra, India and earned the degree of Bachelor of Mechanical engineering in May 2004 with first class. He entered the graduate school at Auburn University in fall 2005 as a graduate student in the Mechanical engineering department.

## THESIS ABSTRACT

### AN EXPERIMENTAL INVESTIGATION OF LIQUID METAL MHPs

Ashish Yudhishthir Palkar

Master of Science, December 17, 2007  
(B.E. Mechanical, PVG's C.O.E.T., University of Pune, 2004)

106 Typed Pages

Directed by Daniel K. Harris

The concept of heat pipes was introduced by R.S.Gaugler in 1940s and Cotter first introduced the idea of “micro” heat pipes in 1984. Cotter in his paper, defined the micro heat pipe as being one in which the mean curvature of the vapor-liquid interface is comparable in magnitude to the reciprocal of the hydraulic radius of the total flow channel. The Micro Heat Pipes (MHPs) work efficiently through the use of two-phase heat transfer. Various working fluids have been tried in combination with various substrate materials. In this experimental work the main focus was to study the behavior of liquid metal filled MHPs made from silicon as the substrate material. Specially designed MHPs were assembled and charged with mercury as the working fluid. A special test setup was designed and built for the experimental work and the response of the MHPs to the controlled increment in the input power is presented.

A number of experiments were carried out on the specimen MHPs to determine their effective thermal conductivity, the variation of the temperature along the axial length and the performance enhancement factor. Effective thermal conductivities as high as 900 W/m-K with a silicon equivalence of 6 were achieved with the liquid metal MHP. Based on the results from the various performance testing parameters, it was observed that the liquid metal charged MHPs performed substantially better than conventional MHPs filled with organic working fluids. The limitations and the possible methods of improving the performance of the MHPs are discussed.

## ACKNOWLEDGEMENTS

I would like to express my gratitude to all those who gave me the possibility to complete this thesis. First of all I would like to thank my advisor, Dr. Daniel K. Harris for his unwavering support and guidance throughout this research work. I would also like to thank my lab mates Omkar Nadgauda and Bhavin Vadgama for their help and valuable inputs.

I am sincerely grateful to my parents and my sister and I would like to take this opportunity to thank them for their unconditional support and love which they have always given me.

Most importantly, I am and will always be grateful to the almighty God.

Style manual or journal used: IEEE

Computer software used: Microsoft Office System 2003, Google SketchUp.



## TABLE OF CONTENTS

LIST OF FIGURES .....	XII
LIST OF TABLES.....	XVI
CHAPTER 1 .....	1
INTRODUCTION .....	1
Heat Pipes .....	1
Heat Pipe Operation.....	3
Micro Heat Pipes (MHPs) .....	4
Need for MHPs.....	5
History of MHPs.....	5
Working Principle of MHPs .....	6
CHAPTER 2 .....	7
LITERATURE REVIEW .....	7
History of the Development of Micro-Heat Pipes (MHPs).....	8
Testing and Analysis of MHPs.....	10
Experimental Work.....	11
CHAPTER 3 .....	35
FACTORS INFLUENCING THE PERFORMANCE OF MICRO HEAT PIPES .....	35
Shape of the Cross Section of MHP .....	35
Working Fluid and Range of Working Temperature.....	36

Operating Temperature.....	39
Charge of the MHP .....	41
Orientation/Angle of Inclination of the MHP.....	42
Length of the MHP .....	44
Heater Size.....	45
Load .....	46
Presence of Non-Condensable Gases .....	47
Contact Angle of the Working Fluid .....	47
Surface Tension of the Working Fluid .....	48
CHAPTER 4 .....	49
THE TESTING OF MICRO HEAT PIPES.....	49
Overview of the Tests.....	49
Testing Approach .....	50
Fabrication of MHPs .....	50
Dimensions of the MHP Used.....	51
Test Setups Used .....	53
Calorimeter .....	55
Calorimeter Insulation .....	57
The Test Parameters .....	58
Charging and Sealing of the MHPs .....	59
Test Procedure .....	61
Performance Testing Parameters .....	63

Results from the Tests Conducted .....	64
CHAPTER 5 .....	83
UNCERTAINTY ANALYSIS .....	83
CHAPTER 6 .....	88
DISCUSSIONS.....	88
Overview .....	88
Conclusion .....	89
Future Work and Recommendations .....	89
BIBLIOGRAPHY.....	91

## LIST OF FIGURES

Figure 1: Cut through view of a conventional heat pipe.....	2
Figure 2: Schematic of a Conventional Heat Pipe. ....	4
Figure 3: Schematic of a micro heat pipe [5].....	9
Figure 4: Temperature profile at an input power of 4 W and sink temperature 15°C [5].....	13
Figure 5: Comparison of the maximum chip temperature for the wafer with and without the micro heat pipe array as a function of input power [5].....	13
Figure 6: Schematic Diagram of Micro Heat Pipes Formed by Vapor Deposition Method [7] .....	14
Figure 7: Centerline Temperature profile for the wafer with the array of 34 heat pipes [7]. ....	16
Figure 8: Centerline Temperature profile for the wafer with the array of 66 heat pipes [7] .....	16
Figure 9: Actual view of vapor phase grooves (top); interface (middle); liquid phase grooves (bottom) [11]. ....	21
Figure 10: Variation of the evaporator temperature as a function of the power input [11].....	22

Figure 11: Variation of the temperature difference between evaporator and condenser as a function of the power input [11] .....	23
Figure 12: Transverse cross-sections of a MHP array (a) with triangular channels (two wafers) and (b) with triangular channels coupled with arteries (three wafers) [8] .....	24
Figure 13: Axial temperature distribution along the pipe length for various fluid fill charges for the triangular channel MHP array (symbols: experimental curves and line: calculated curve) [8]. ....	27
Figure 14: Axial temperature distribution along the pipe length for the MHP array with arteries either charged or empty (symbols: experimental curves and line: calculated curve) [8].....	27
Figure 15: Temperature distribution measurements along the micro heat pipe for different input-power levels [12]. ....	28
Figure 16: Relationship between effective thermal conductivity $K_{eff}$ , Length $L$ and Hydraulic diameter $D_h$ , as given by Badran and Gerner et al. [3].....	30
Figure 17: $K_{eff}$ versus power input for 100 $\mu m$ , water, 15°C sink temperature [3] .....	32
Figure 18: $K_{eff}$ versus power input for 100 $\mu m$ , methanol, 15°C sink temperature [3] .....	32
Figure 19: $K_{eff}$ versus power input for 260 $\mu m$ , water, 10 ° C sink temperature [3]. ....	33

Figure 20: Keff versus power input for 260 $\mu\text{m}$ , methanol, 10 ° C sink temperature [3].	33
Figure 21: Dependence of thermal performance of MHP on the operating temperature [14].	40
Figure 22: MHP array effective thermal conductivity as a function of the liquid fill ratio for methanol, ethanol, and pentane [19]	41
Figure 23: Schematic showing the angle of inclination of a heat pipe.	42
Figure 24: MHP –base, lid and the heating element in the groove on the lid....	52
Figure 25: 3-D model of the first test setup used (without the insulation cover).	54
Figure 26: 3-D model of the Calorimeter used in final test setup (without the insulation cover).	56
Figure 27: Calorimeter with the insulation cover.	57
Figure 28: MHP array die and its components---lid and the base.	60
Figure 29: Graph showing the variation of difference between evaporator and condenser temperature with respect to power input, for various tests conducted.	65
Figure 30: Graph showing the variation of the evaporator temperature with the change in the power input.	66
Figure 31: Graph showing the variation of equivalent thermal conductivity, calculated using silicon equivalence method, versus input power. (S/W=Silicon/water and S/M=Silicon/Mercury).	70
Figure 32: MHP base dimensions.	71

Figure 33: Comparison of the effective thermal conductivity versus input power, for various MHPs.....	72
Figure 34: Thermal resistance vs. the input power for various MHPs74	
Figure 35: Comparison of various MHPs using the average effective thermal conductivity76	
Figure 36: Comparison of various MHPs in terms of improvement of ‘Keff’ over the empty MHP (enhancement factor).....	77
Figure 37: Comparison of the results from the two methods used to calculate the thermal conductivity. ....	78
Figure 38: Actual MHP size comparison.....	81
Figure 39: Test setup.....	82
Figure 40: Uncertainty analysis performed on the three MHPs.....	87

## LIST OF TABLES

Table 1: The end temperatures of evaporator and condenser and the improvement of the heat conductivity for various heat inputs [11]. .....	19
Table 2: Summary of literature review. ....	34
Table 3: Range of operating temperature for some common heat pipe working fluids [16]. .....	37
Table 4: Variation of critical heat input (W) with inclination ( $\theta$ ) for a V shaped micro heat pipe of length 2 cm [22]. ....	43
Table 5: Calculation of equivalent thermal conductivity, based on silicon equivalence approach. ....	69
Table 6: Comparison of the heat flux through MHP (S/W= Silicon/Water, S/M=Silicon/Mercury). ....	75
Table 7: Silicon Thermal Conductivity [30]. ....	79
Table 8: Mercury Thermal conductivity [30]. ....	80



## CHAPTER 1

### INTRODUCTION

#### Heat Pipes

A heat pipe can be defined as a simple device that can transfer heat from one end to its other end at relatively high rates. Another definition states that a heat pipe is a heat transfer device that can transport relatively large quantities of heat over a small temperature gradient between its ends. Heat pipes are therefore considered an effective means to transfer thermal energy. Although a heat pipe is similar to a thermosyphon, it differs from a thermosyphon by virtue of its ability to transport heat against gravity by an evaporation-condensation cycle with the help of porous capillaries that form the wick. It is the wick which provides the capillary driving force to return the condensate back to the evaporator.

The basic components of a typical heat pipe are:

- The container— main body of the heat pipe.
- The wick structure.
- The working fluid.

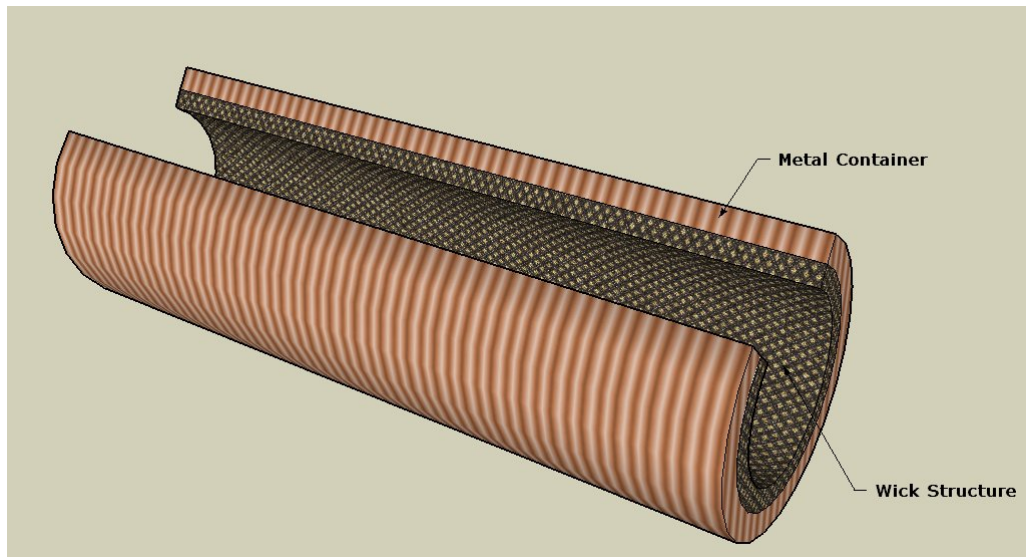


Figure 1: Cut through view of a conventional heat pipe.

The container material of the heat pipe is typically copper or aluminum, but may differ according to the application for which the heat pipe is used. Similarly the choice of the material for the wick structure and the working fluid also depends on the application. Since heat pipes don't have any moving parts, they require no maintenance. Therefore, heat pipes are also referred to as 'passive' devices and they do not require pumps or other mechanical actuators to make them work.

One of the characteristics of heat pipes is their ability to maintain constant evaporator temperatures under varying heat flux levels. Also, because heat pipes utilize the closed two-phase cycle, their thermal response time is considerably less than those for other types of heat transfer devices.

## Heat Pipe Operation

The capacity of heat pipes to transport large amounts of heat, from a warmer end to a cooler end, comes from a two phase heat transfer mechanism employed in their working. The working of heat pipes is primarily driven by the temperature difference between its hot and cold ends.

When one end of the heat pipe is heated, the working fluid inside the pipe at that end (evaporator) evaporates; which increases the vapor pressure inside the cavity of the heat pipe. The difference between the vapor pressure at the evaporator end and the equilibrium pressure at the condenser end causes a pressure gradient in the vapor core that causes the vapor to travel towards the condenser end of the heat pipe. At the condenser end, the excess vapor condenses and releases its latent heat, which in turn, raises the temperature of the cooler end of the heat pipe. The condensed liquid is absorbed into the wick structure and flows back, due to the capillary pressure within the wick, towards the evaporator end for evaporation.

Thus, the thermal energy is transferred from the warmer (evaporator) end to the cooler (condenser) end as the working fluid vaporizes upon absorbing the latent heat of evaporation at the evaporator end, and condenses back to liquid form at the condenser end. This process continues in a cyclic manner thereby facilitating the working of the heat pipe without any external driving force. Following is the schematic diagram of a heat pipe.

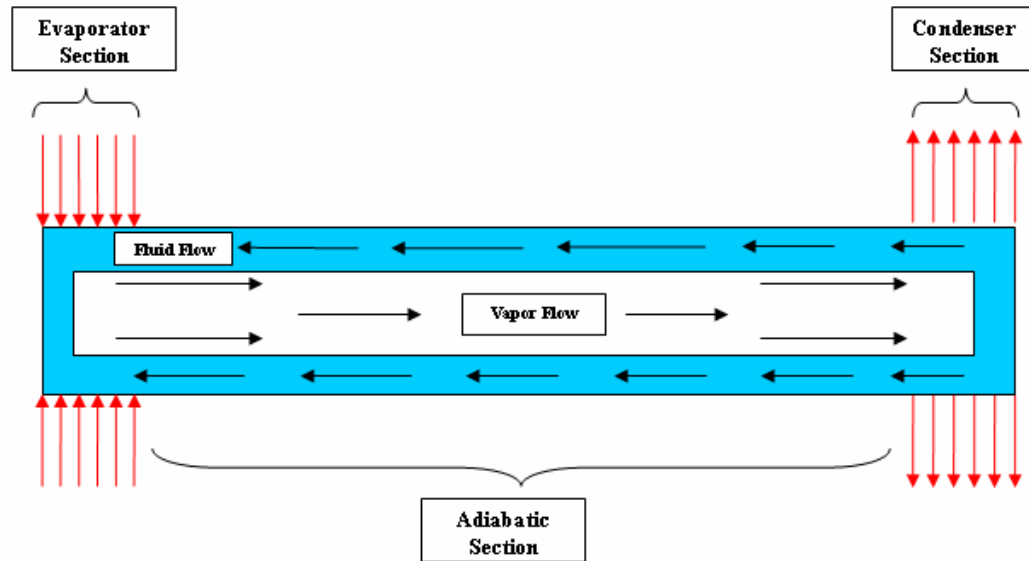


Figure 2: Schematic of a Conventional Heat Pipe.

### Micro Heat Pipes (MHPs)

Heat pipes are available in various shapes and sizes. They vary from sizes as big as a 15 m long monogroove heat pipe developed for spacecraft heat rejection, to as small as a few millimeters (5 to 10) long, which are used for applications in the semiconductor industry. Based on the lengths, they can be roughly categorized as regular heat pipes, mini heat pipes and micro heat pipes. One distinguishing difference between the regular heat pipe and a micro heat pipe is that a micro heat pipe does not have a wick structure to facilitate the return of the working fluid from the condenser end to the evaporator end. Instead, it uses the capillary forces generated in its sharp edges of the cross section.

## Need for MHPs

Due to their characteristic small sizes, micro heat pipes are well suited to the semiconductor industry. Micro scale heat pipes were proposed for use in removing heat from laser diodes and other small localized heat generating devices, the thermal control of photovoltaic cells, the removal or dissipation of heat from the leading edge of hypersonic aircraft, and even in the medical field to remove cancerous tissues through hyper or hypothermia [1].

The micro heat pipe, which acts as a two-phase heat exchanger combines the advantage of high latent energies, associated with phase change and advance micro-fabrication technique. Thus, with the advancement of the manufacturing process in the semiconductor industry, it has even become possible to incorporate micro heat pipes in the same substrate as that of the electronic chip.

## History of MHPs

The concept of heat pipes was introduced by R.S. Gaugler in 1940's. But, it was in 1984 that Cotter first introduced the idea of "micro" heat pipes [2]. Since then many researchers have contributed to the understanding and development of the micro heat pipes.

## Working Principle of MHPs

Cotter in his paper, defined the micro heat pipe as being one in which the mean curvature of the vapor-liquid interface is comparable in magnitude to the reciprocal of the hydraulic radius of the total flow channel. In an attempt to better comprehend the definition of MHPs given by Cotter, Babin *et al.* (1990) expressed Cotter's definition in mathematical form [2] given by equation (1.1).

$$K \propto 1/rh \quad (1.1)$$

Where K is the mean curvature of the liquid-vapor interface and rh is the hydraulic radius of the flow channel. Peterson then developed a dimensionless expression by assuming a constant of proportionality of 1 and multiplying both the mean curvature of the liquid-vapor interface and the hydraulic radius by the capillary radius  $r_c$ . Thus, he obtained:

$$r_c / rh \geq 1 \quad (1.2)$$

The fundamental principles of operation of micro heat pipes are the same as those of the conventional larger version of heat pipes. As stated earlier, one major difference is the absence of the wick structure in MHPs, which is present in the conventional heat pipes.

## CHAPTER 2

### LITERATURE REVIEW

Due to the recent developments in semiconductor technology, it is possible to produce miniature devices which have very high levels of performance. This has in turn led to an increase in the power densities, increased thermal gradients and higher mean operating temperatures. The issue of heat dissipation from thermal devices has been gaining more attention in the recent past. Conventional techniques of cooling and heat dissipation are not sufficient enough to handle these increased power densities and constant research work is going on to develop effective and efficient solutions to these thermal problems.

Heat pipes, which are devices of very high thermal conductance, are one of the many techniques which have been successfully implemented in the industry. It was not until its independent invention by G.M. Grover in the early 1960's that the remarkable properties of the heat pipe became appreciated and serious developmental work began [3].

As the semiconductor industry develops, electronic components and devices of smaller dimensions and higher performance are manufactured. Therefore, better electronic cooling and thermal management techniques are always in demand. It is needed to modify and further develop the existing heat pipe technology so as to cater to the needs of increasing thermal loads and higher power densities. Thus, the option of micro heat pipes was investigated as a possible solution for compact devices which are built to the mini and micro scales. A micro heat pipe (MHP) is a small-scale device that uses the latent heat of phase change (from liquid to vapor and vice versa) to dissipate energy from a heat source [4].

Silicon micro heat pipe arrays are passive micro-cooling systems used to transfer high heat fluxes and to increase the effective thermal conductivity of the silicon substrate. The role of a MHP is to reduce the maximum temperature of the wafer, to decrease the temperature gradient across the wafer and thus to increase the effective thermal conductivity [5] .

### History of the Development of Micro-Heat Pipes (MHPs)

Investigations such as those by Tuckerman and Pease (1981) showed that large amounts of heat can be dissipated using rectangular channels etched or cut into the chip, through which a liquid is pumped. The technique provided a significant increase in the cooling capacity and achieved good temperature uniformity over the chip surface.



With the design, fabrication and testing of ultra-compact, water cooled, plate-fin heat sinks, Tuckerman and Pease (1981) found that these micromechanical heat sinks were capable of dissipating  $4W/cm^2$ . The heat sinks consisted of  $300\ \mu m$  by  $50\ \mu m$  rectangular channels, with  $100\ \mu m$  inter-channel spacing and were cooled by forced convection of water. Shortly after this, Cotter (1984) proposed the concept of a “micro-heat pipe”. A micro heat pipe is a wickless, non-circular channel with a diameter of  $10\ \mu m$  to  $500\ \mu m$  and a length of about  $10\ mm$  to  $20\ mm$  [6]. Figure 3 shows a schematic of a micro heat pipe.

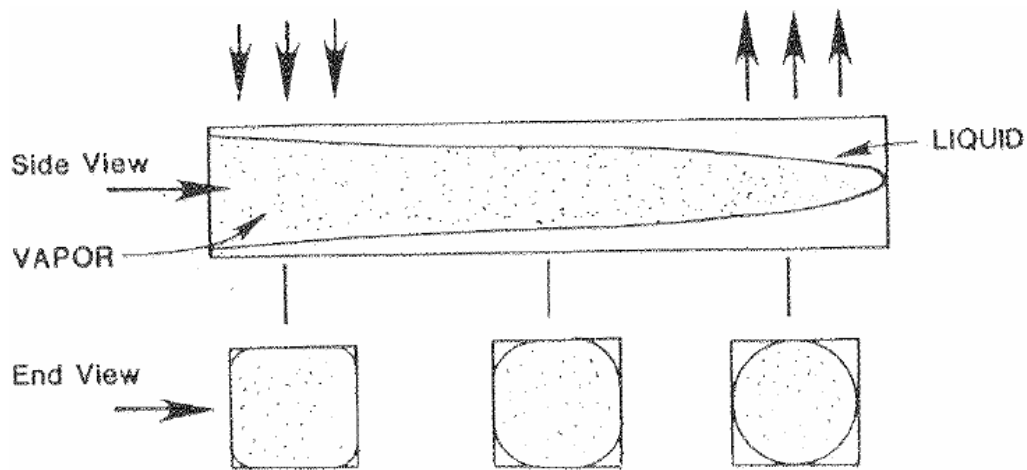


Figure 3: Schematic of a micro heat pipe [6]

Micro heat pipes etched in to silicon substrates have been studied in detail and with interest because such heat pipes are very compact, very light and have better hydraulic behavior than the metallic heat pipes [7].

Weichold *et al.* (1993) suggested that fabrication of an array of vapor deposited micro heat pipes as an integral part of silicon wafer can be an alternative technique for providing temperature uniformity over the wafer surface [8].

## Testing and Analysis of MHPs

Many researchers and scientists have tested and analyzed the performance, behavior and limitations of micro heat pipe arrays. Some of the many materials of construction used for micro heat pipes are copper, silver, stainless steel and silicon. Silicon is one of the commonly used substrates for the fabrication of the micro heat pipe arrays. Also different working fluids have been tried. The choice of the working fluid depends upon the range of the working temperature and the application of the micro-heat pipes. Deionized water, methanol, ethanol and pentane are some of the commonly used working fluids.

The investigations of the micro heat pipe arrays can be broadly classified into two categories viz. theoretical and experimental. A number of mathematical models have been developed and studied for the analysis of micro heat pipe arrays and the results have been compared to the experimental data collected from testing carried out on actually fabricated MHPs.

The fabrication of the micro heat pipe array roughly consists of three operations: the machining of a series of channels of predetermined dimensions into the silicon wafer, the bonding process and finally the heat pipe charging.

The normal Si-Si direct bonding process described [9] is as follows: Si-Si direct bonding, allows the most intimate integration of two entities without external forces such as an electric field or an adhesive layer. The wafers are first dipped in HF to remove the native oxide on the surface, cleaned in piranha ( $\text{H}_2\text{SO}_4:\text{H}_2\text{O}_2$ ) and RCA ( $\text{NH}_4\text{OH}:\text{H}_2\text{O}_2:\text{H}_2\text{O}$ ) for 15 min each, and then spin dried. Cleaning in piranha and RCA solutions is known to remove organic and metallic surface contamination while rendering the Si surface hydrophilic.

Hydrophilic wafers are bonded after the drying process. Following this pre-bonding at room temperature with the cover wafer, the wafers are annealed at  $1100^\circ\text{C}$  for 1 hour in order to obtain a sufficient strong interfacial bonding strength. The bonding quality is then inspected using infrared transmission imaging.

## Experimental Work

G.P.Peterson and A.B.Ducan *et al.* (1991) conducted a series of tests on an array of 39 parallel rectangular channels,  $30\text{ }\mu\text{m}$  wide,  $80\text{ }\mu\text{m}$  deep and  $19.75\text{ mm}$  long, which were machined into a silicon wafer  $2\text{ cm}^2$  and  $0.378\text{ mm}$  thick with an inter-channel spacing of  $500\text{ }\mu\text{m}$ . An ultraviolet (UV) bonding process was used to bond the channel containing silicon wafer to a glass cover.

For the bonding purpose, a thin layer of an ultraviolet sensitive adhesive, Norland Optical Adhesive 81 was used. The adhesive was cured by exposure to an ultraviolet light source with a wavelength range between  $320\text{ nm}$  and  $380\text{ nm}$  for approximately 150

seconds and then allowed to cure for an additional twelve hours. Methanol was used as the working fluid and the test results of the micro heat pipe arrays were compared to the results from a plane un-grooved wafer. The heater was located on the side of the wafer opposite the heat pipe array, so as to match the actual application. The power to the heaters was supplied by a Kepco model ATE 36-8M power supply.

The voltage and current to the heaters was measured by two digital multimeters. The input power to the heaters could be determined to within  $\pm 0.05$  Watts. The experiment was conducted to verify the heat pipe concept and determine the potential advantage of constructing an array of micro heat pipes as an integral part of semiconductor devices.

The authors concluded that the results indicate that incorporating an array of micro heat pipes as an integral part of semiconductor chips can significantly decrease the temperature gradient across the chip, decrease the maximum chip temperature and also the number and intensity of localized hot spots. For silicon wafers with a micro heat pipe array density of 1.24 % and power levels of  $4 W / cm^2$ , reductions in the maximum chip temperature of approximately 11 °C and increases in the effective thermal conductivity of approximately 25 % were measured. [6]. These results are presented in the form of graphs in Figure 4 and Figure 5.

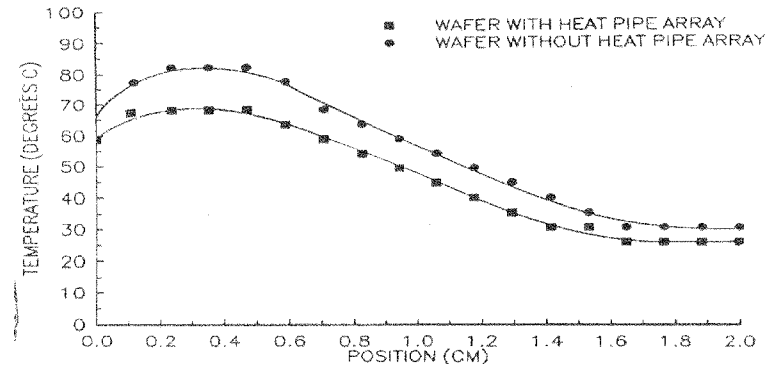


Figure 4: Temperature profile at an input power of 4 W and sink temperature 15°C [6].

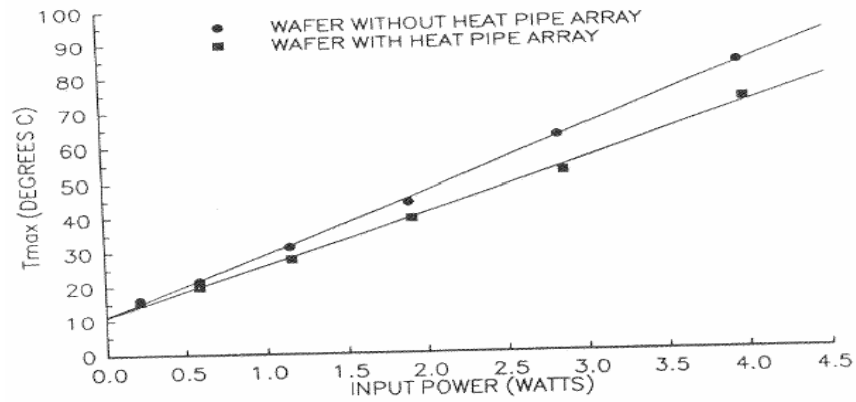


Figure 5: Comparison of the maximum chip temperature for the wafer with and without the micro heat pipe array as a function of input power [6].

Other experiments conducted (Peterson and Ducan 1991, mentioned above) showed that the incorporation of micro heat pipe arrays in the silicon wafer had many advantages like decrease in maximum chip temperature and increase in the thermal conductivity. But, it was noticed by Peterson *et al.* (1993) that there was a problem with the migration of the working fluid into the silicon. As a solution to these problems, the use of the new technique called the ‘vapor deposition technique’ was suggested.

The construction of the micro heat pipes, using the vapor deposition technique, was accomplished by first establishing a series of parallel grooves in a silicon wafer. Then, a thin layer of metal (30  $\mu\text{m}$ ) was deposited over the grooves using a combination of pre-deposition (described by Mallik *et al.* 1993) to close the grooves. This resulted in a series of small triangular grooves, each lined with a layer of metal to prevent migration of the working fluid into the silicon wafer. Once fabricated, the heat pipes were evacuated, charged and sealed [8] .

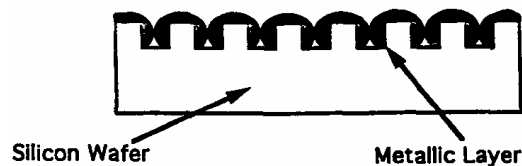


Figure 6: Schematic Diagram of Micro Heat Pipes Formed by Vapor Deposition Method [8].

Mallik and Peterson [8] carried out an experiment on an array of vapor deposited micro heat pipes. It consisted of 34 and 66 triangular, parallel, vapor deposited micro heat pipes, each 25  $\mu\text{m}$  wide and 55  $\mu\text{m}$  deep. These two arrays occupied a percentage cross sectional area of 0.75 and 1.45 respectively. The working fluid used was methanol.

For the array of 34 micro heat pipes, reduction in the maximum surface temperature and maximum temperature difference of 24.4 % and 27.4 % respectively were reported for  $4.70 \text{ W} / \text{cm}^2$ .

The effective thermal conductivity of this array increased from 165.66 W/m-K at an input of 0.5 W to a value of 181.46 W/m-K at an input power of 3.02 W. The improvement in the effective thermal conductivity was approximately 47 percent for a heat flux of  $4.70 \text{ W} / \text{cm}^2$  [8].

Similarly, for the array of 66 heat pipes, the maximum surface temperature increased linearly from 15.2 °C for a power of 0.10 W to 87.2 °C for a power input of 3.5 W. The reduction in maximum surface temperature and the maximum temperature difference were equal to 29 % and 33.3 %, respectively, for a heat flux of  $4.70 \text{ W} / \text{cm}^2$ . The effective thermal conductivity increased from 165.66 W/m-K at an input heat flux of  $0.78 \text{ W} / \text{cm}^2$  to a value of 186.27 W/m-K at an input heat flux of  $4.70 \text{ W} / \text{cm}^2$ . This was greater than a 50 % improvement in the effective thermal conductivity [8]. Figure 7 and Figure 8 plot the temperature profiles.

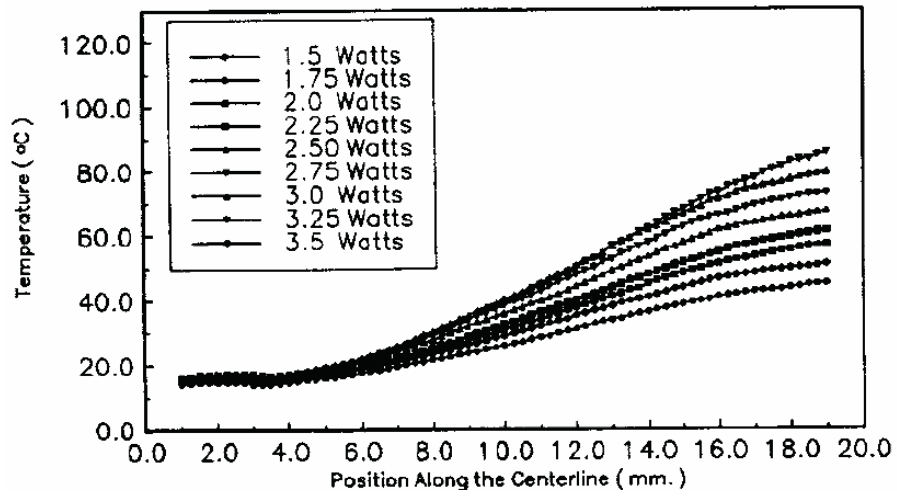


Figure 7: Centerline Temperature profile for the wafer with the array of 34 heat pipes [8].

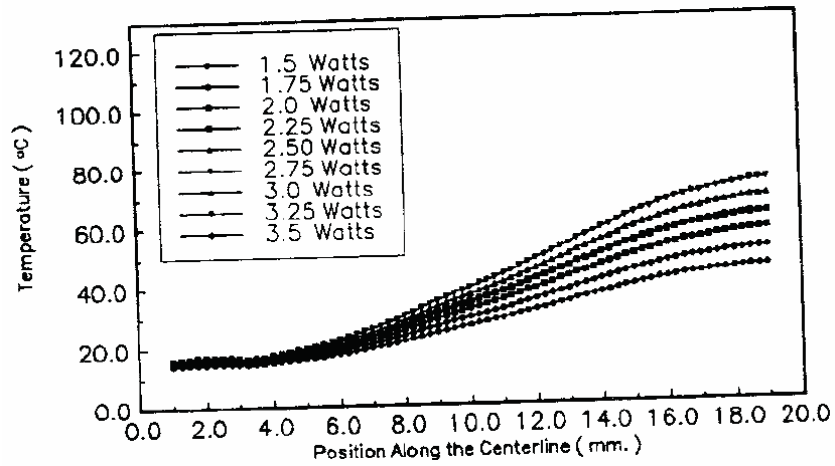


Figure 8: Centerline Temperature profile for the wafer with the array of 66 heat pipes [8].



Wu and Peterson [10] conducted tests on the heat pipe originally modelled by Babin *et al.* They did so to verify the transient model developed to investigate the micro heat pipes. The experiments were carried out on silver micro heat pipes with dimensions approximately 1mm (D) by 2mm (W) and 60 mm in length. They were charged with 0.032g of ultra pure deionized water. In this experiment two separate techniques for measuring the temperature were employed. One of them consisted of a series of eight Special Limit of Error (SLE) copper-constantan (AWG 36) thermocouples with a measurement uncertainty of  $\pm 0.5$  °C.

The second technique used an infrared thermal measurement system. A Hughes Probe Eye TVS Model 3000 Infrared Camera in conjunction with a RGB monitor and a real time recorder were used to observe the temperature profile of the test pipe during both the startup and the steady-state operation. They observed that the vapor temperature variations were proportional to the heat input and that without dry out or flooding, the effective conductivity of the heat pipe was independent of time shortly after start-up. But the other thermal parameters required fairly long times to reach their steady state values. The most interesting result of the numerical modeling effort was the behavior of the liquid in the corner regions. The reverse liquid flow, predicted by the model, during the startup was hypothesized to be the result of an imbalance in the overall pressure drop, i.e. because the evaporation rate does not provide a sufficient change in the liquid-vapor interfacial curvature adequate to compensate for the total pressure drop resulting from the temperature change.

It was also observed that as the power level increased, the heat pipe began to operate more efficiently and the axial temperature drop remained constant. This phenomenon was similar to that observed in very short heat pipes. At low powers they were relatively inefficient due to the thermal resistance of the case, wick etc., but as the length increased the advantage became more apparent [10].

In 2001 J.S. Park and J.H. Choi *et al.* reported their findings [11] from the tests conducted on flat micro heat pipe arrays with 38 triangular grooves. Each triangular groove had the dimensions of 100  $\mu\text{m}$  (W), 70  $\mu\text{m}$  (D) and 15 mm (L).

The heater was fabricated using the Cr/Au evaporation, had an area of 66  $\text{mm}^2$  and covered up to 5 mm from the end of the heat pipe arrays. Degassed deionized water, 20 % charge (by volume), was used as the working fluid. Eight T-type thermocouples connected to a Yokogawa DA2500E data acquisition system were used for temperature measurement. The power supply used was an HP6674. The authors mentioned that when the heat was not dissipated externally at steady state, the heat flux is the same as the heat input. Accordingly, the reciprocal of temperature gradient (temperature difference) was construed as the heat conductivity of a heat pipe. The test results showed an improvement of 25 % to 33 % in the thermal conductivity. Following table, Table 1, summarizes the test results as given by the authors.

Input power	Temp. of empty FMHP (°C)			Temp. of FMHP filled (°C)			Improvement of heat conductivity
	Evaporator	Condenser	Temp. difference	Evaporator	Condenser	Temp. difference	
1.9W	61.5	30.6	30.9	56.7	33.5	23.2	33.2%
3.5W	89.8	34.5	55.3	84.8	40.8	44.0	25.7%
4.9W	117.5	39.2	78.3	109.0	47.2	61.8	26.7%
5.9W	139.2	43.3	95.9	127.1	52.2	74.9	28.0%

Table 1: The end temperatures of evaporator and condenser and the improvement of the heat conductivity for various heat inputs [11].

In 2002 Shung-Weng Kang *et al.* performed tests on radially grooved micro heat pipes, using deionized water as the working fluid. Fabrication of the radial grooved MHP in this study required three masks, for the upper vapor phase grooves structure, the middle interface, and the lower liquid phase grooves structure. Figure 9 shows the actual view of these three grooves. The vapor phase grooves were trapezoidal in shape, 23 mm in length, with 70 grooves in total spreading in a radial manner from the center outward. The width at the inner end of a groove was 350  $\mu\text{m}$  and the width at the outer end of groove was 700  $\mu\text{m}$ . There were 16 grooves for alignment during eutectic bonding and a mouth at the center for suction purposes during the filling process. The liquid phase grooves were trapezoidal in shape, 23 mm in length and the width at inner and outer ends was 150  $\mu\text{m}$  and 500  $\mu\text{m}$  respectively.

The distribution was similarly radial with 70 grooves and 16 grooves were for alignment purpose. The mask at the central portion was octagon in shape with four supporting pillar structures. The hollow portion was for the connection between the vapor phase and liquid phase.

For the radial MHPs of this experiment, an Au–Si eutectic bonding was used with optical fiber alignment technique to form the three pieces of the structure into one body. After completion of etching of the MHP, the three wafers were placed into BOE solution to remove the oxide layer residue. After rinsing with deionized water, a solution of 3:1 volume mixture of vitriol and hydrogen peroxide was used to clean the wafer surface, followed by rinsing with deionized water and blowing with nitrogen to dry the wafer. Subsequently the wafer was placed in an electron beam evaporating machine at a deposition rate of 5 Å° and 25 Å° per second, to evaporate a layer of 75 Å° of Cr and 2000 Å° of Au.

Then using the long-shaped alignment groove formed with the previous mask design, a 520 µm diameter optical fiber was inserted into the groove as stop. After the three wafers were aligned, the combination was placed into a diffusion bonding chamber and the body was evacuated to vacuum before applying 0.5 to 1  $kg/cm^2$  bonding pressure and control the time and temperature at each section [12].

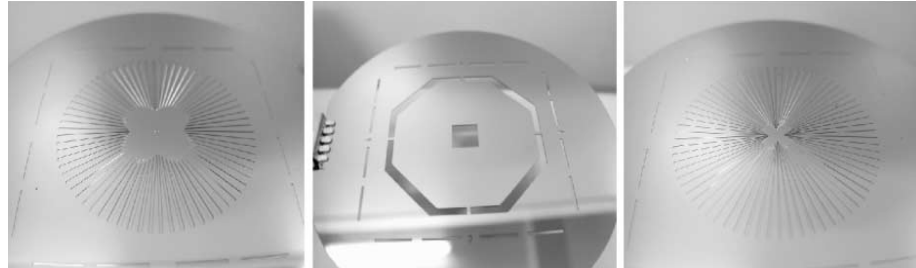


Figure 9: Actual view of vapor phase grooves (top); interface (middle); liquid phase grooves (bottom) [12].

The MHP of this study used pure silicon as the base material and water as the working fluid. The wettability of silicon with water is not good and causes a decrease of capillary action; therefore an evaporated gold layer was used during bonding to form a eutectic reaction.

As the wettability of gold with water is better than that of silicon, the capillary pumping force was significantly enhanced. Arrangements were made in this experiment to individually measure the top surface and bottom surface temperature of the micro heat pipes, so as to obtain the required surface temperature difference. 16 K-type (Omega TT-K-40) thermocouples were used, which were connected to the Omega OMB-1100 data acquisition system.

A Topward 6303D power supply was used to provide power to the heater and the voltage and current were measured using digital multimeters. To minimize the heat loss, the heater assembly was insulated using styrofoam insulation.

Omegatherm 204, a high thermo-conductivity coefficient paste, was used to increase the adhesion and reduce the contact resistance of the thermocouples. The variation of the evaporator surface temperature as a function of the power input is shown in Figure 10 below. The highest temperature occurred for the plain wafer. For an input power of 27 W the temperature for the plain wafer was about 92 °C, whereas the temperatures for the wafers with 30 % and 53 % fill ratio were about 84.9 °C and about 73.4 °C respectively. The wafer with 70 % fill ratio had the lowest evaporator surface temperature of 67 °C.

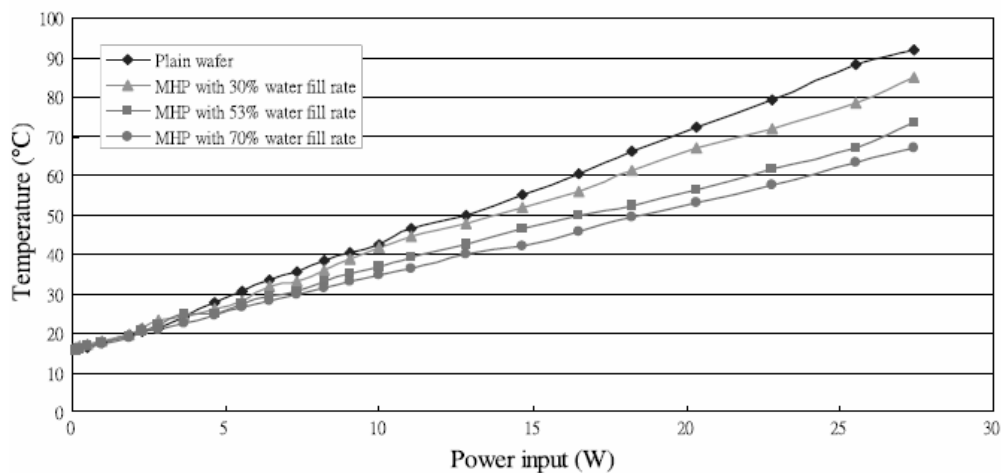


Figure 10: Variation of the evaporator temperature as a function of the power input [12].

Figure 11 shows the variation of the temperature difference between evaporator and condenser as a function of the power input. The temperature difference between evaporator and condenser section was about 47 °C with 70 % fill rate. This value was lower than plain wafer structure by 33 % [12].

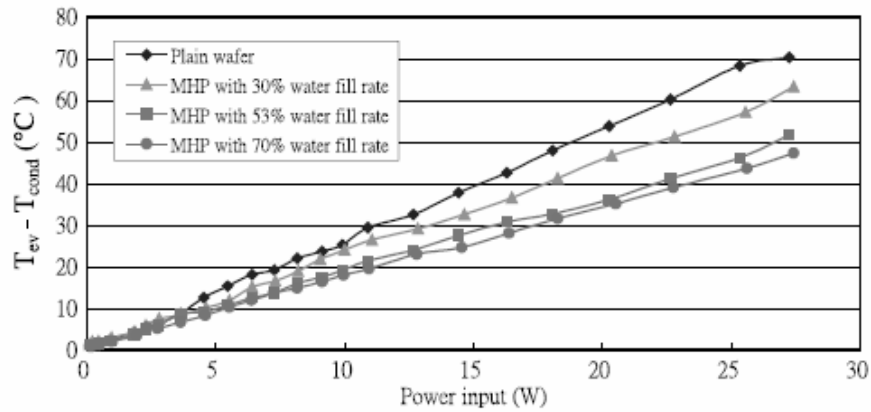
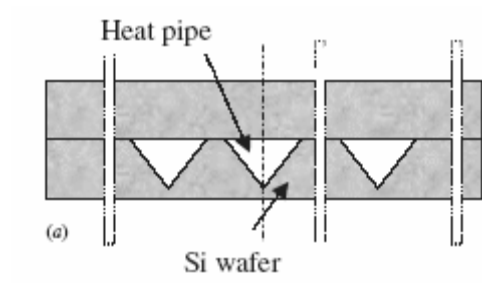


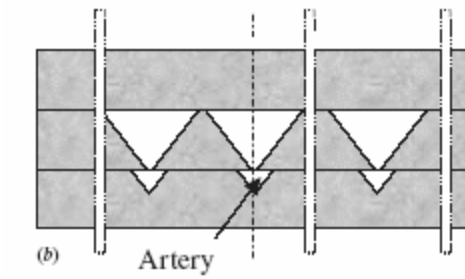
Figure 11: Variation of the temperature difference between evaporator and condenser as a function of the power input [12].

The authors reported that for 27 W, the highest employed fill rate of 70 % showed the best performance with the evaporator temperature 27 % lower than that of the plain wafer.

M Le Berre, S Launay, V Sartre and M Lallemand [9] carried out experiments on two types of micro heat pipe arrays and reported their results in 2003. The first type of arrays consisted of 55 parallel heat pipes (triangular in shape, each 230 μm wide, 170 μm and 20 mm long) and the other, 25 parallel heat pipes (triangular in shape with artery, each 500 μm wide, 170 μm and 20 mm long).



(a)



(b)

Figure 12: Transverse cross-sections of a MHP array (a) with triangular channels (two wafers) and (b) with triangular channels coupled with arteries (three wafers) [9].



One of the objectives of this study was to provide experimental data to determine the extent to which, the two types of MHP arrays can reduce the maximum temperature of the wafer, decrease the temperature gradient across the wafer and thus increase the effective thermal conductivity. Ethanol was the working fluid for a 55 MHP array (3W) and methanol was used as the working fluid for an array with 25 MHP (2W). Fill charges from 0 % up to 66 % were tested. It is mentioned by the authors that methanol should be preferred to ethanol because of its higher merit number,  $4.3 \times 10^{10} \text{ W} / \text{m}^2$  instead of  $2.1 \times 10^{10} \text{ W} / \text{m}^2$  respectively, at 50°C. Merit number is defined by equation (2.1)[3]

$$M' = \rho_l^2 L k_l^3 / \mu_l \quad (2.1)$$

where M = merit number

$\rho_l$  = liquid density

L = latent heat of vaporization

$K_l$  = liquid thermal conductivity

$\mu_l$  = liquid viscosity.

T-type thermocouples placed on a kapton tape were used to measure the temperature distribution under ambient temperature. The experimental accuracy in temperature measurement was estimated to be  $\pm 0.2K$ .

The authors observed that there was a systematic slight temperature decrease of the charged 55 MHP array as compared to the empty MHP array for fill charges between 6 % and 66 % and whatever heat input between 0.5 W and 4 W. However this temperature discrepancy was found to be close to the experimental uncertainty and therefore no significant heat transfer enhancement could be clearly proved.

These results were found to be close to the experimental results of Badran *et al.* [4] according to whom, the improvement due to silicon MHP array was negligible as the major part of heat was transferred by conduction in the silicon. This was due to the low void fraction, about 8 % of the MHP cross section. And, it was suggested that the geometry of the MHP be improved and optimized. In the second half of the experimental work, the authors examined the working of the MHP with arteries.

The effective thermal conductivity evaluated by the 3D simulation was found to be 600 W/m-K, which represented an increase of 300 % of the silicon thermal conductivity. The void fraction for the MHP arrays with arteries was reported to be 15 % and the enhancement due to the MHP was therefore found to be noticeable. The experimental findings of this group are graphically represented in Figures 13 and 14.

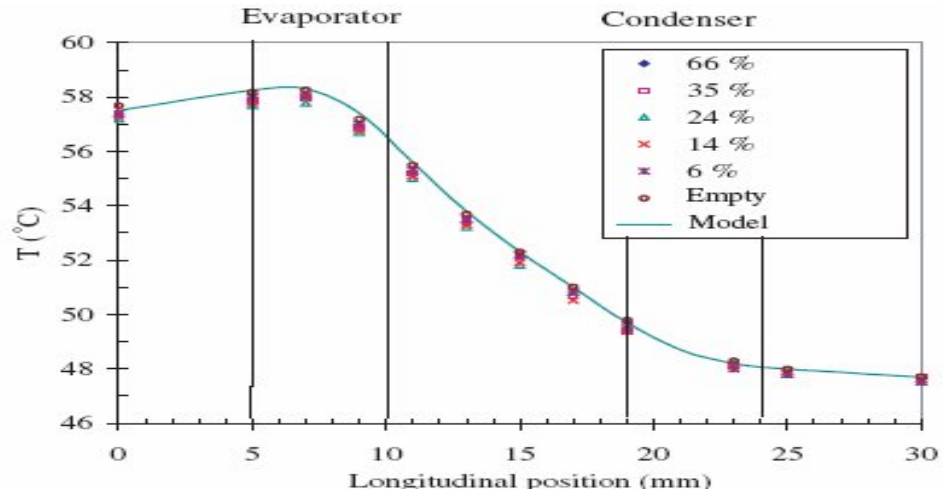


Figure 13: Axial temperature distribution along the pipe length for various fluid fill charges for the triangular channel MHP array (symbols: experimental curves and line: calculated curve) [9].

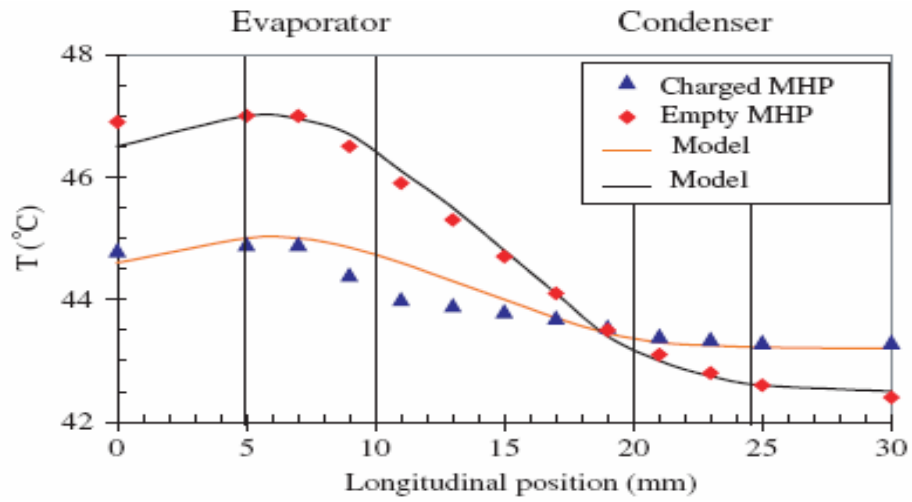


Figure 14: Axial temperature distribution along the pipe length for the MHP array with arteries either charged or empty (symbols: experimental curves and line: calculated curve) [9].

In 2002 Man Lee, Man Wong and Yitshak Zohar tested a micro heat pipe system which consisted of four heat pipes with triangular cross sections. Each pipe was 100  $\mu\text{m}$  wide, 20 mm in length and had a hydraulic diameter of 52  $\mu\text{m}$ . deionized water was used as the working fluid. The heater and temperature sensors were fabricated within the silicon substrate by selective doping using standard surface micromachining techniques. The output signals from the temperature microsensors were collected using a computerized data acquisition system. Figure 15 summarizes the temperature distribution along the MHP for different input power levels.

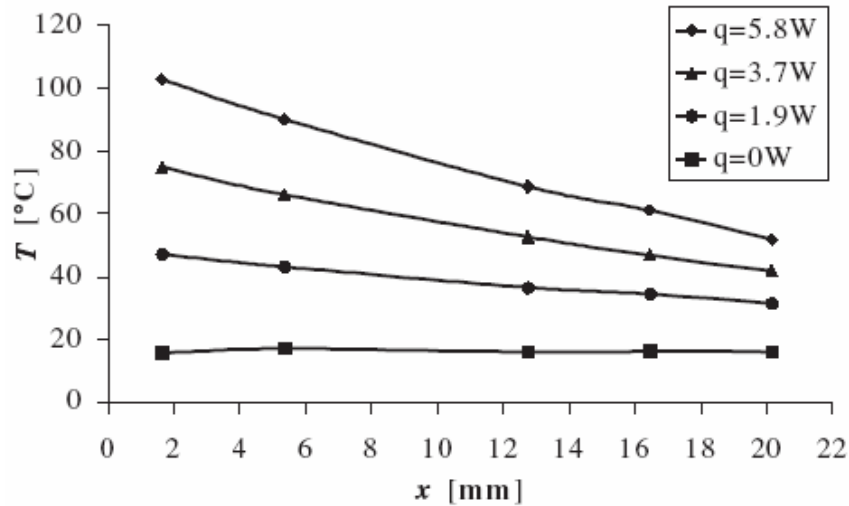


Figure 15: Temperature distribution measurements along the micro heat pipe for different input-power levels [13].

It was noted that the increasing negative temperature gradient along the heat pipe is due to the higher rate of input heat flux in comparison with the rate of thermal conduction along the microdevice [13].

B.Badran and F.M.Gerner *et al.* [4] investigated the working of silicon micro machined micro heat pipes at low temperatures using water and methanol as the working fluid. They published their experimental results in 1997. The experimental facility built by them was used to verify the operation of two arrays of MHPs on a semiconductor silicon wafer. The individual MHP had an isosceles triangle cross section with a length of 25.4 mm and a width of 100  $\mu\text{m}$  and 260  $\mu\text{m}$ , and various filling charges of 5 %, 10 %, 20 %, 30 %, 50 % and 80 % were tested.

K-type thermocouples, connected to the data acquisition system, were used to measure the temperature and Fourier's law was used to calculate the effective thermal conductivity. A Kapton flexible 20 mm by 2 mm, 33  $\Omega$  heater was used and was glued to the evaporator section.

The authors acknowledged that in their experimental work, the silicon micromachined MHP had a large thermal mass (relative to the size of the MHP) which acted as a conductor and hence the case may not be considered isothermal. But, it was stated that although the conduction in the silicon MHP was large, the main aim was to evaluate and compare the effective thermal conductivity of the heat spreader array filled and unfilled with the working fluid. This was to prove the operation of the MHP array as a heat spreader.

The model used was basically a thermal resistance model and it predicted the thermal conductivity,  $K_{\text{eff}}$ , of the silicon/working fluid MHP wafer. It was found by the authors that the effective thermal conductivity was inversely proportional to the width, i.e. the hydraulic diameter of the pipe, and directly proportional to the length of the

MHP. The model used was one-dimensional and took only the axial conduction along the MHP into consideration. The relationship was presented in the form of a graph, which is as shown in Figure 16.

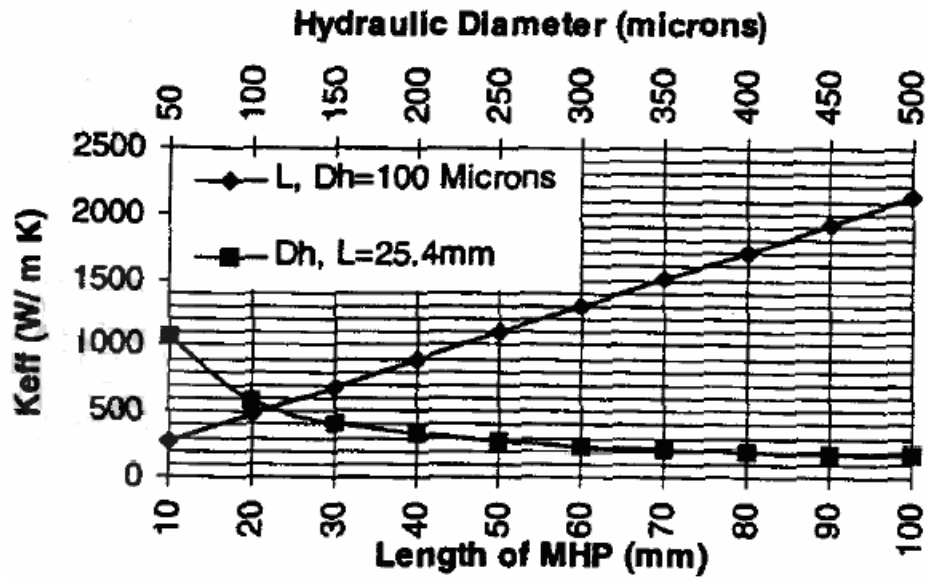


Figure 16: Relationship between effective thermal conductivity  $K_{eff}$ , Length  $L$  and Hydraulic diameter  $D_h$ , as given by Badran and Gerner *et al* [4].

For the purpose of testing, two sets of MHPs were fabricated. The first array of MHPs consisted of 73 MHPs, which were 260  $\mu\text{m}$  wide and had depth of 185.54  $\mu\text{m}$ . The second set of MHP array fabricated was 127 in number, had a width of 100  $\mu\text{m}$  and a depth of 70.72  $\mu\text{m}$ .

The cross sectional void (the ratio of the cross sectional area occupied by the MHP array to the silicon cross sectional area based on a 0.0257 m by 0.0254 m surface area) was established as approximately 25 % for the 260  $\mu\text{m}$  wide pipe and approximately 6 % for the 100  $\mu\text{m}$  wide pipe.

The array of MHPs occupied a center surface area of 0.0254 m by 0.0254 m (1 in. by 1 in.). The authors mentioned that the justification for the use of the Fourier equation in their work was that, although the thermal conductivity may not be accurately predicted, the performance of filled and unfilled micro heat pipes could be compared for effective thermal conductivity and evaporator temperature. The authors also made a note of the suggestion by Cao and Faghri that for Knudsen numbers less than 0.01 a large axial temperature gradient exists, which leads to lower effective thermal conductivities.

It was reported that the temperature of a water/silicon micro heat pipe must be above 40  $^{\circ}\text{C}$  for the pipes to function [4]. It was concluded that the MHP arrays showed an improvement of about 6 % and 11 % using methanol and water as the working fluid, respectively, at high power levels. A 5 % fill quantity was established for proper functioning of a MHP. It was concluded that the reason for the small improvement in the experimental work might be due to the large thermal conductivity of silicon. For an improvement of 10 %, the effective thermal conductivity for the 260  $\mu\text{m}$  wide pipe was theoretically calculated as 229 W/m K, which was smaller than expected. The conjugate model predicted much higher performance of almost 10 times more than observed in the experimental work of the authors.

The following graphs show the variation of the Keff with respect to power inputs, for the two different working fluids and the two different types of the MHP arrays. Table 2 summarizes the literature review.

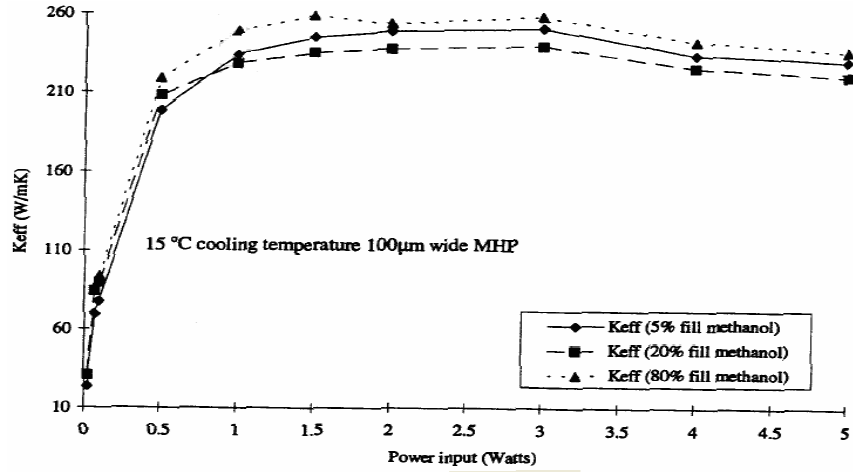


Figure 17: Keff versus power input for 100 μm, water, 15 °C sink temperature [4].

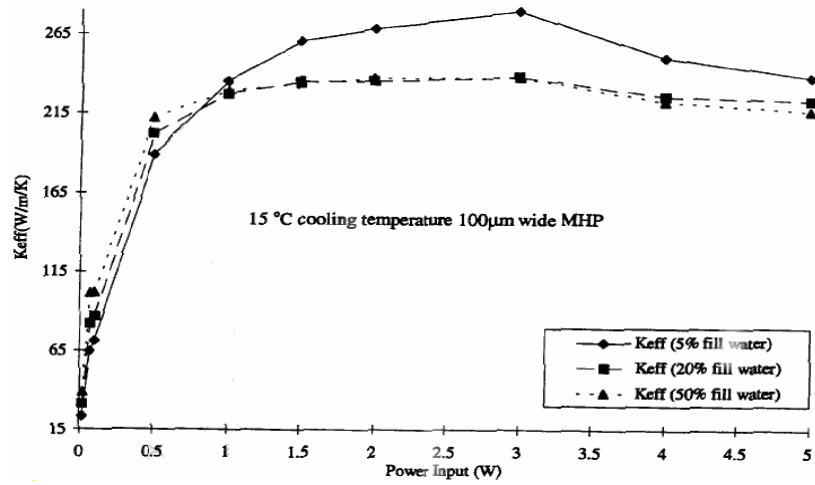


Figure 18: Keff versus power input for 100 μm, methanol, 15 °C sink temperature [4].



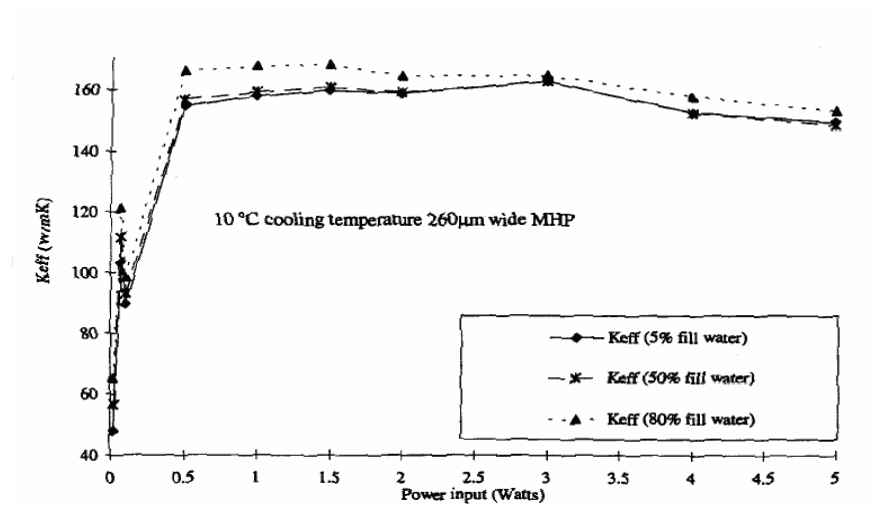


Figure 19: Keff versus power input for 260 μm, water, 10 °C sink temperature [4].

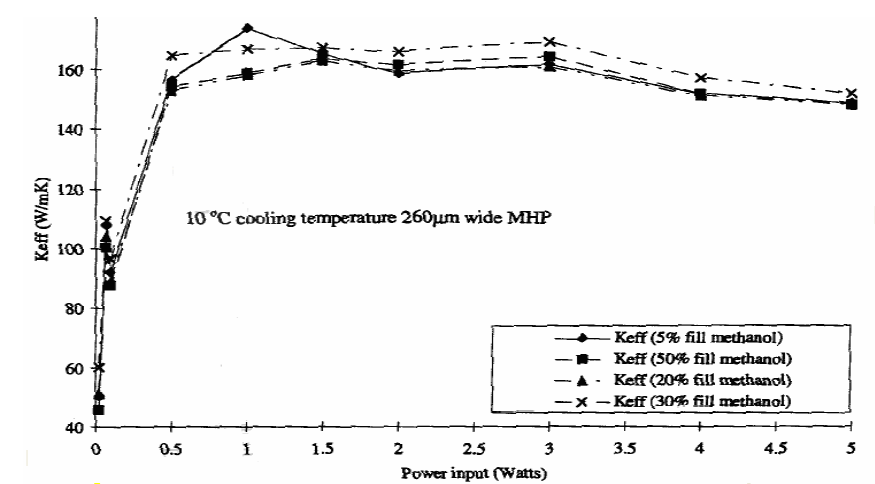


Figure 20: Keff versus power input for 260 μm, methanol, 10 °C sink temperature [4].

Authors	Cross Section	No. of Channels	Working Fluid	Power (W)	$\Delta T$ (°C)	Substrate Material	Method of Analysis	Year
Peterson G.P, A.B.Duncan,A.S Ahmed,A.K.Mallik M.H.Weichold	Rectangular	39	Methanol	4	35	Silicon	Experimental	1991
A.K.Mallik & G.P.Peterson	Triangular	34 & 66	Methanol	3.5	65 & 59	Silicon	Experimental	1995
Bassam Badran, Frank M Gerner,Padmaja Ramadas,Thuman Henderson and Karl W.Baker	Triangular	-	Water and Methanol	-	-	Silicon	Experimental	1997
Sivaraman Anand, Sirshendu De & Sunando Dasgupta	Triangular	-	Pentane	1.52	10	Silicon	Experimental	1999
Park, J.S; Choi, J.H.; Cho, H.C.; Yang, S.S.; Yoo, J.S.	Triangular	38	D.I. Water	1.9 to 5.9	23.2 to 74.9	Silicon	Experimental	2001
Man Lee,Man Wong & Yitshak Zohar	Triangular	4	D.I. Water	5.8	~50	Silicon	Experimental	2002
Shung-Weng Kang,Sheng- Hong Tsai & Hong-Chih Chen	Trapezoidal (raidal)	70	D.I.Water	5	10- 12	Silicon	Experimental	2002
M Le Berre, S Launay, V Sartre & M Lallemand	Triangular and Triangular with arteries	55& 25	Ethanol and Methanol	3 & 2	10 & 1.5	Silicon	Experimental	2003
A.Lai,C.Gillot, M.Ivanova,Y.Avenas,C.Louis, C.Schaeffer,E.Fournier	Rectangular	-	D.I.Water	11	~16	Silicon	Experimental	2004
Balram Suman, Sirshendu De & Sunando DasGupta	Triangular	10	Pentane	0.5, 2 & 3	1,4 & 6	Silicon	Theoretical	2004
Balram Suman & Prabhat Kumar	Triangular and Rectangular	-	Pentane	1.52	~9	Silicon	Theoretical	2005
MLeBerre, Guillaume Pandraud, Pangiota Morfouli & M Lallemand	Triangular	27	Methanol	3	~9	Silicon	Experimental	2006

Table 2: Summary of literature review.

## CHAPTER 3

### FACTORS INFLUENCING THE PERFORMANCE OF MICRO HEAT PIPES

#### Shape of the Cross Section of MHP

As discussed earlier, a micro heat pipe (MHP) is normally a non-circular channel with a hydraulic diameter of 10-500  $\mu\text{m}$ . It has been found that for the heat pipe to operate satisfactorily, it is necessary to have sharp angled corners in the micro heat pipe. The meniscus recession in the evaporator region causes a reduction in the meniscus curvature radius, which in turn causes an increase in the capillary pumping pressure [9]. Thus it is important for a MHP to have a sharp edge in the corners for making the working fluid return from the condenser to the evaporator.

Although channels of any polygonal cross-section where the corners are capable of developing the required capillary action for circulation of the working fluid can act as micro heat pipe channels, the fabrication method utilized imposes the major limitation in the geometric design of channels. The most widely used cross-sectional shapes as fabricated on substrates are: trapezoidal, triangular and rectangular cross-sections [14].

The rectangular MHP with curved sides has an advantage for thermal performance [15] such as larger inner space for vapor flowing and one more corner for liquid path than those of a triangular MHP.

Since the edge angle at the corner of the triangular MHP is sharper than that of the rectangular MHP, the capillary force of the working fluid at the triangular MHP is larger than that at the rectangular MHP [15] .

### Working Fluid and Range of Working Temperature

The choice of the working fluid depends mainly on the working temperature range. Various fluids have been used for charging of the micro heat pipes. Table 3 summarizes some of the common working fluids used in heat pipes and their respective working temperature ranges.

Working Fluid	Temperature Range
Hydrogen	-258 to -244 C (-433 to -408 F )
Nitrogen	-213 to -175 C (-351 to -283 F)
Methane	-184 to -130 C (-300 to -202 F)
Freon	-79 to 27 C(-110 to 81 F)
Ammonia	-61 to 13 C (-78 to 56 F)
Freon	-36 to 88 C (-32 to 190 F)
Water	39 to 164 C (102 to 328 F)
Mercury	237 to 486 C (458 to 907 F)
Cesium	454 to 927C (850 to 1700F)
Potassium	532 to 1021 C (990 to 1870 F)
Sodium	649 to 1149 C (1200 to 2100 F)
Lithium	1032 to 1654 C ( 1890 to 3010 F)

Table 3: Range of operating temperature for some common heat pipe working fluids [16].

D. Sugumar and Tio Kek Kiong studied MHPs filled with three working fluids viz: water, ammonia and methanol. They observed the effects of the properties of these working fluids on the heat transport capacity. The study was confined to the temperature range of 20 °C to 100 °C. It was reported that they observed the behavior of heat transport capacity to be dominated by a property of the working fluid, which was equal to the ratio of the surface tension and dynamic viscosity ( $\sigma/\mu$ ). This property has the same dimension as the velocity, and can be interpreted as a measure of the working fluid's rate of circulation which is provided by capillarity pressure above that need to overcome the viscous effects.

The numerical results of the study of the working fluids showed that ammonia yielded the highest heat transport capacity for a micro heat pipe in the temperature range of 20 °C to 50 °C. But, it was also observed that the performance of ammonia filled MHPs deteriorated in terms of heat transport capacity when the operating temperature exceeded 50 °C. The authors concluded that, among the working fluids studied, water was the best choice in the temperature range of 20 °C to 100 °C as it yielded the highest heat transport capacity of the micro heat pipe. [17]

Apart from the factor of suitable working temperature range, the selection of working fluid also depends on other factors which are important to the performance of the heat pipe.

Some of the desired characteristics of a suitable working fluid for the MHP are as follows:

- a. The fluid should be compatible with the material of the MHP.
- b. It should have good thermal stability, should wet the walls of the MHP.
- c. The vapor pressures should not be too high or too low over the operating temperature range.
- d. The liquid should have high latent heat.
- e. High liquid thermal conductivity.
- f. Low liquid and vapor viscosities.
- g. High surface tension.

## Operating Temperature

The performance of a MHP is affected by the operating temperature and the control of the MHP's working temperature is important for its optimum performance. It was reported by D.Sugumar and Kek Kiong Tio [18] that a micro heat pipe will operate effectively by achieving its maximum possible heat transport capacity only if it is to operate at a specific temperature—the design temperature.

They observed that when a MHP is operated at a higher temperature than the design temperature, the heat transport capacity increases but is limited by the onset of dryout at the evaporator section. On the other hand, the heat transport capacity decreases if it is to be operated at lower temperatures than the design temperature due to the occurrence of flooding at the condenser end.

Similar findings were reported by Kek-Kiong Tio *et al.*, in their paper [19]. They concluded that the heat transport capacity of a MHP increased, with the operating temperature higher than that of the temperature for which the MHP was optimally filled. In such a case, the maximum achievable rate of heat transport would be limited by the onset of dryout.

On the other hand, the heat transport capacity was concluded to diminish if the MHP operated below the temperature for which it was optimally filled and the limiting factor in this case being the onset of flooding at the condenser end.

S.H.Moon *et al.* studied the relation between the operating temperature and the thermal performance of the MHP. Figure 21, from their work [15], presents experimental thermal resistance and the heat transfer limit of a triangular MHP for various operating temperatures. The tested MHP had a fill ratio of 20 % and was tested for the various operating temperatures of 60, 70, 80, and 90 °C.

As shown in the Figure 21, the heat transfer limit was a function of the operating temperature and increased as the operating temperature increased. The heat transfer limits were 6.18, 7.59, 8.01, and 10 W for the operating temperatures of 60, 70, 80, and 90 °C, respectively [15] .

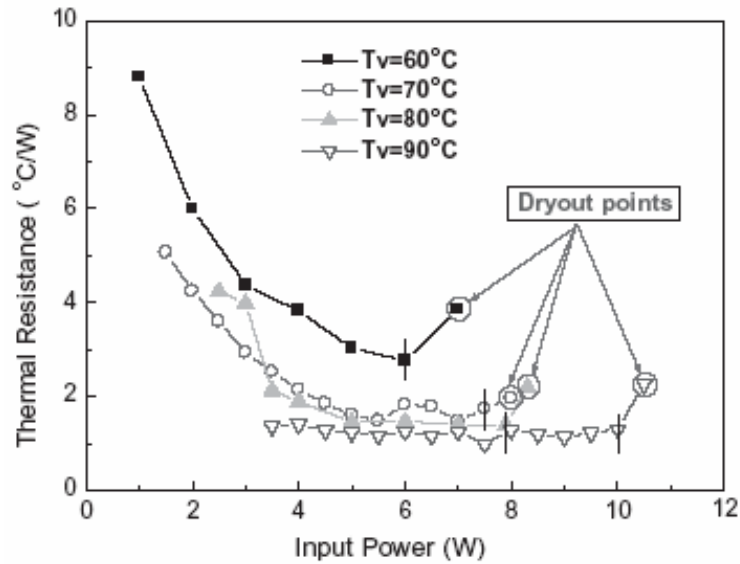


Figure 21: Dependence of thermal performance of MHP on the operating temperature [15].



## Charge of the MHP

The charge of the micro heat pipe is the amount of the working fluid filled into the MHP and is an important factor in defining the performance of the MHP. The fill ratios normally range from very low values to values as high as 60 % to 70 % by weight. Pandraud and Le Berre *et al.* in their experimental work [20] on five different working fluids determined the relationship between the fill ratios and the performance of MHP. They reported that the best performances of MHPs were recorded with lower fill ratios rather than with high fill ratios. This relationship is expressed in the form of a graph, shown in the Figure 22.

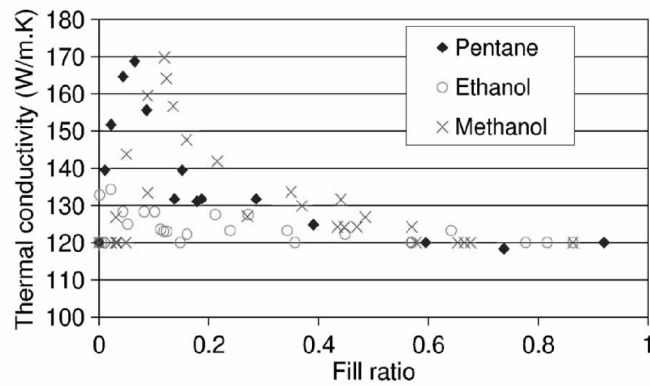


Figure 22: MHP array effective thermal conductivity as a function of the liquid fill ratio for methanol, ethanol, and pentane [20].

## Orientation/Angle of Inclination of the MHP

The orientation of the MHP is defined by the angle of the evaporator and condenser sections with respect to the gravity horizontal. If the condenser is placed at an elevated position in comparison the evaporator, it is considered to be a positively oriented MHP and the angle of inclination is recorded with a positive sign.

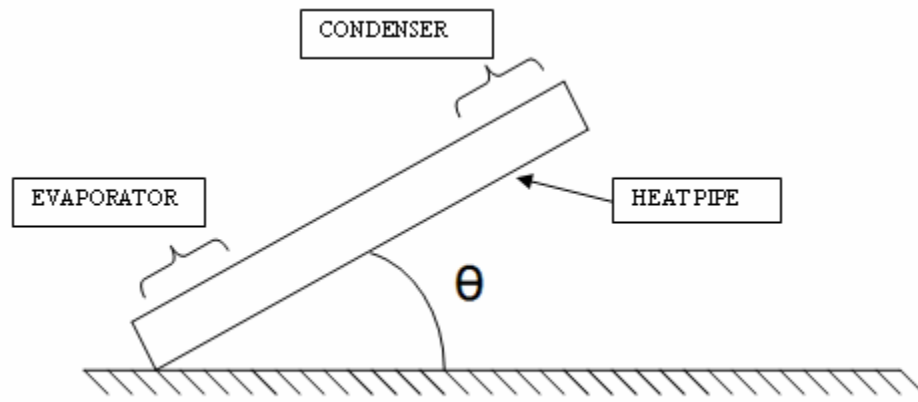


Figure 23: Schematic showing the angle of inclination of a heat pipe.

D. Sugumar and Kek-Kiong Tio [21], reported that for an inclined micro heat pipe, the heat transport capacity is also limited by the simultaneous onsets of dryout and flooding and that for such MHP, gravity can either enhance or inhibit the performance, depending on its orientation. They observed and reported that for a constant operating temperature of 60 °C with water as the working fluid the allowable heat transport rate of the micro heat pipes increased with an increase in angle of inclination.

It is known that if the other factors such as the shape and geometry of the MHP are maintained constant, the heat transport capacity of a horizontal micro heat pipe is provided mainly by its working fluid's ability to circulate effectively.

Thus, it is seen that for a positively inclined micro heat pipe, the additional driving agent of the gravitational force enhances the circulation rate of the working fluid and therefore causes the increase of the allowable heat transport rate [21].

Balram Suman and Nazish Hoda reported that the critical heat inputs of a heat pipe vary significantly with its inclination. With the increase in the inclination of the heat pipe, the critical heat input decreased and was due to the opposing effect of the body force [22].

Inclination (°)	Critical heat input (W) $\times 10^2$
0	1.24
10	1.15
30	0.94
45	0.84
60	0.78
90	0.72

Table 4: Variation of critical heat input (W) with inclination ( $\theta$ ) for a V shaped micro heat pipe of length 2 cm [22].

It was reported that the capillary limit would be reached earlier for a heat pipe with a higher inclination angle. Also, the rate of change of critical heat input with respect to the inclination was found to decrease with increase in inclination [22].

## Length of the MHP

The length of the micro heat pipe is one of the critical parameters governing its performance. It has been found that the longer the heat pipe is the lower is the critical heat input. This can be explained by the fact that the friction loss is larger in a longer heat pipe. Thus, with an increase in length of a heat pipe, the performance has been observed to decrease. Balram Suman and Nazish Hoda found from their work on MHPs that the rate of change of critical heat input with respect to length decreases with increase in length [22].

G.P. Peterson and H.B. Ma in their paper [23] have stated that “when the length of a micro heat pipe increases, the heat transfer capacity decreases and not only does the unit effective area heat transfer decrease, but so too does the total heat transfer”.

Seok Hwan Moon *et al.*, in their experimental work, found that the overall heat transfer coefficient for triangular MHPs, for the same thermal load of 3 W, was enhanced by about 92 % when the total length of the MHPs was reduced from 100 mm to 50 mm. [15]

Balram Suman, in his paper states [24], “The higher the heat pipe length, the lower the performance factor. This is explained by the fact that with an increase in the length of a heat pipe, the frictional loss increases.” Thus the performance of the MHP is critically dependant on its length.

As suggested by Cao, Y, A. Faghri *et al.* in their work [25] when the size of the heat pipe decreases as in the case of the micro heat pipe, it may encounter vapor continuum limitations.

This limitation may prevent the micro heat pipe from working under lower temperatures. But, for a heat pipe operating at higher working temperatures, this limitation is temporary and will disappear when the heat pipe temperature increases. Also, the maximum heat flux based on the conventional formulation is on the order of  $10 \text{ W} / \text{cm}^2$ , which is relatively low. However, since the size of a micro heat pipe is very small, the disjoining pressure may help to increase the heat transport capacity of the heat pipe. The disjoining pressure results from the repulsion of the vapor phase by the solid and the liquid from the long range intermolecular forces [25]. The authors suggested that further study was needed to quantify this effect.

### Heater Size

Srikaran Kalahasti and Yogendra K. Joshi conducted tests on a novel flat plate micro heat pipe spreader. Among the various parameters investigated by them in their study, leading geometrical, material and boundary parameters of the spreader were considered. They reported that for any power level, as the heater size was reduced, the heat flux in the evaporator region increased drastically.

This caused a dramatic jump in the spreader peak wall temperature. The authors tested three different heaters with 3 mm, 6 mm and 7.5 mm sizes. In the case where the heater size was 3 mm, the maximum peak temperature was observed, and it illustrated the extreme sensitivity of the heat spreader to the evaporator size.

From the study it was seen that the ratio of the heater length to the overall spreader length was an important parameter controlling the resistance to spreading of heat from the heater to the condenser section. The smaller the heater, the more critical the hot spot formation, and higher the peak wall temperature. Hence they suggested that it would not be advisable to employ ‘small’ heat spreaders for removing heat from extremely small sections. [26]

## Load

S.H. Moon *et al.* have mentioned in their work [15], the effect of increasing the thermal load on the performance of the MHP. With the increase in the thermal load, the vapor flow velocity increases.

Thus, the friction force on vapor-liquid interface and the pressure drop in the liquid flow are increased. The authors state that since the space for the vapor flow in the MHP is narrower than that in the conventional heat pipe, the pressure drop by the friction on vapor-liquid interface may largely affect the performance of MHP. [15]

## Presence of Non-Condensable Gases

The presence of non-condensable gases can be detrimental to the performance of the micro heat pipes. Since these gases can not condense, they cause a reduction in the area of condensation and thus lead to the reduction in the heat transfer from the condenser region [27].

In 1961, Sparrow and Eckert showed that, as little as 0.5 percent by mass of non-condensable gases in the vapor phase can reduce the heat transfer by about 50 % [27]. The size of the micro heat pipe is significantly small and thus, the presence of the non-condensable gases has a magnified effect because they have an effect on the phase change mechanism.

## Contact Angle of the Working Fluid

The contact angle between the working fluid and the substrate is an important factor in deciding the performance of the MHP. Even a small increase in the contact angle can significantly improve the performance of the MHP [22].

As the contact angle increases, more liquid can fit in the smaller groove and thus more working fluid is available for evaporation, this improves the performance of MHP. Therefore, this factor of contact angle is considered while selecting a working fluid for the MHP.

## Surface Tension of the Working Fluid

Balram Suman and Nazish Hoda have mentioned in their work [22], that the higher the surface tension of the working fluid, the greater is the pressure difference between the liquid-vapor interface and thus, better is the pumping action of the fluid from the condenser end to evaporator end, thereby giving a greater MHP performance.



## CHAPTER 4

### THE TESTING OF MICRO HEAT PIPES

#### Overview of the Tests

The testing of the micro heat pipes (MHPs) was carried out to determine their performance. The test results were used to compare the performance of charged MHPs filled with working fluids such as water or mercury with the performance of an uncharged specimen. Measurements were made to determine how effectively the charged specimen of the MHPs reduced the temperature variation over their length for a given heat input at the evaporator end and heat sink temperature at the condenser end. The collected data was then reduced and compared to the data from similar works done by other research groups.

## Testing Approach

In order to incorporate the practical working conditions and to make the analysis of the collected data less complex, certain assumptions were made. It was verified that the convective heat losses from the MHP and its test setup to the surrounding were minimized by the use of a proper insulation cover. Steady state operation of the MHP during the testing was verified.

## Fabrication of MHPs

The micro heat pipes used in this study were fabricated from two wafers. On one of the wafers, the base of the MHP containing the 22 micro channels was etched and on the other the lid for the MHP was fabricated. Single side polished wafers were used in the fabrication of the channels. The orientation of the wafer was 100 or 110. The thickness of the wafers was 300  $\mu\text{m}$  and the wafers used were 4 inches in diameter.

The micro heat pipes were fabricated in the Alabama Micro Science and Technology Center (AMSTC) in Auburn University. Layers of titanium, nickel and indium were deposited on the wafers with the e-beam evaporator at thicknesses of 500  $\text{\AA}$ , 300  $\text{\AA}$  and 10,000  $\text{\AA}$  respectively. The wafers were then deposited with layers of titanium, platinum and gold at thickness of 100  $\text{\AA}$ , 1000  $\text{\AA}$  and 150  $\text{\AA}$  respectively using an e-beam machine [28].

Indium was used for bonding, but since it does not adhere to silicon very well, it had to be deposited on a thin layer of nickel. A layer of titanium was used so as to make nickel to adhere to silicon. The platinum layer was supported by a titanium layer. Gold layer was used as a sacrificial layer since mercury amalgamized the gold layer and then wetted platinum in its purest form [28].

DRIE (Deep Reactive Ion Etching) was used to form the channels with the vertical walls. This process is a highly anisotropic etch process used to create deep/steep sided holes or trenches in wafers with aspect ratio of 20:1 or more. An anisotropic etch is one which attacks certain crystal planes much more rapidly than others and produces etch cavities with flat surfaces that intersect each other at sharp well defined angles [29].

#### Dimensions of the MHP Used

The channels had a square cross section, 100  $\mu\text{m}$  wide 100  $\mu\text{m}$  deep and were 9500  $\mu\text{m}$  in length. There were 22 channels in each die with a 100  $\mu\text{m}$  pitch. The ratio of the area occupied by the 22 channels to silicon cross sectional area (the area of the whole chip) was approximately 0.3654 and thus, the cross sectional void was calculated to be approximately 36.5 %.

A groove was etched on the top side of each lid in order to allow for the placement of the heating element (tungsten filament). The groove was 250  $\mu\text{m}$  deep, 1000  $\mu\text{m}$  wide and five millimeters long. It was made at a distance of one millimeter from one of the shorter edges of the lid, as shown in Figure 24.

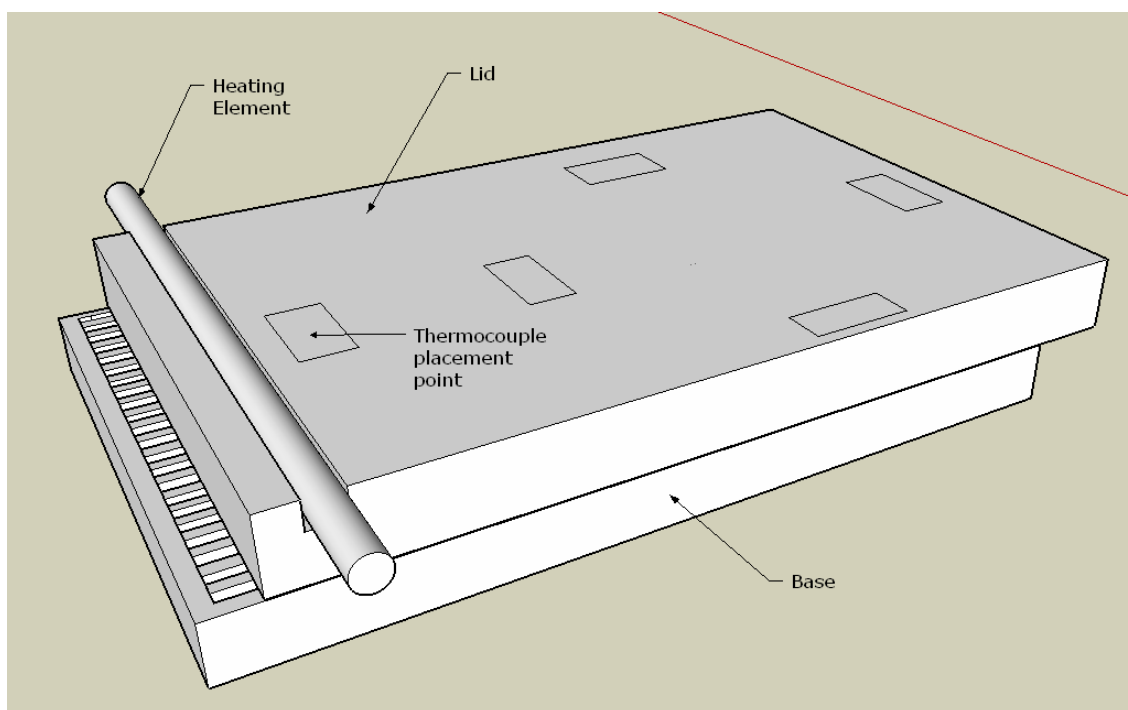


Figure 24: MHP – base, lid and the heating element in the groove on the lid.

## Test Setups Used

One of the important factors which helps in evaluating the performance of the MHP is its response, in terms of the temperature change, to a varied heat input. Thus, it was required to measure the temperature variation along the axial length of the micro heat pipe array for various power inputs.

The experiments on the MHP array required a test setup which could support the test die of the MHP array with its heating element, the connecting wires and the two temperature sensing thermocouples placed on the top face of the die.

Also, it was required to facilitate the cooling of the MHP array die by establishing a path for the heat to flow from the MHP to the cold plate, which acted as a constant temperature heat sink. The first test setup consisted of the test specimen micro heat pipe, the heating element (tungsten wire) mounted in the groove of the micro heat pipe and connecting wires, and thermocouples (OMEGA K-type) mounted on the MHP, a variac, a cold plate, the AGILENT 34970A data acquisition system, a digital multimeter and an ammeter.

The MHP die was mounted on a metal plate of suitable size (copper plate approximately 30 mm by 25 mm) using Norland Electronic Adhesive 121. The metal plate was then pasted onto the cold plate using CHEMPLEX 1381, a silicon based grease like material specially blended with thermally conductive fine metal oxide powders to provide high thermal conductivity and high temperature stability.

A thin film heat flux sensor, manufactured by Omega Engineering (HFS-4), was attached at the lower side of the metal plate such that it was positioned between the metal plate and the cooling plate.

The flux sensor was used to evaluate how much of the applied heat was actually going through the MHP. The heat flux sensor had dimensions of 2.85 cm by 3.51 cm and had a built in K-type thermocouple. The setup was covered up with a thermal insulation layer so as to minimize the convective losses to the surroundings. Figure 25 is a model showing the first type of the test setup, without the insulation cover.

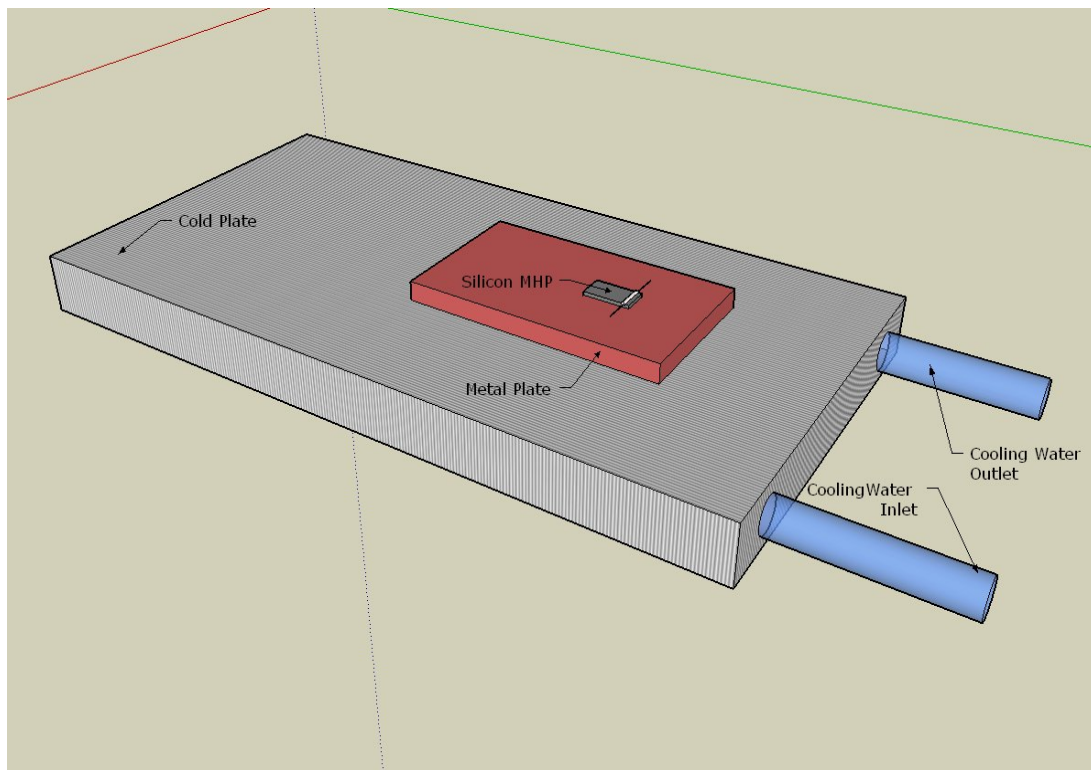


Figure 25: 3-D model of the first test setup used (without the insulation cover).

In the second test setup, a calorimeter was used. The method of mounting the MHPs on the calorimeter was preferred to the method of direct mounting of the MHP on to the cold plate using a copper plate. This was because the calorimeter provided a better means to measure the heat going through the MHP. The calorimeter was manufactured to have precise dimensions and the dimensions were accurately measured to calculate the required cross sectional area. This also helped in calibrating the calorimeter. The calorimeter was mounted with four RTDs along its square cross sectional column at a measured interval of 5 mm. The figure of the calorimeter (Figure 26) given in the following section will assist in understanding the above given explanation.

### Calorimeter

The calorimeter was made up of aluminum (6061 T6). It was calibrated and the calibration correction constant determined. The calibration correction from applied electrical power to the amount of energy traversing the calorimeter cross section was determined to be 87 %. This was very consistent with most of the in-house measurements. Therefore, it was concluded that a 13 % heat loss was associated with parasitic heat transfer along the sensor wires and through the insulation. The top face of the calorimeter was dimensioned so as to closely match the dimensions of the die containing the MHP array. Its length was 10 mm and the width was 5 mm.

The column of the calorimeter was made slender with a square cross section, of side 5.007 mm. The cross sectional area of the calorimeter was thus well known. Also, the temperature along its height could be measured at four equi-spaced points using four embedded RTDs.

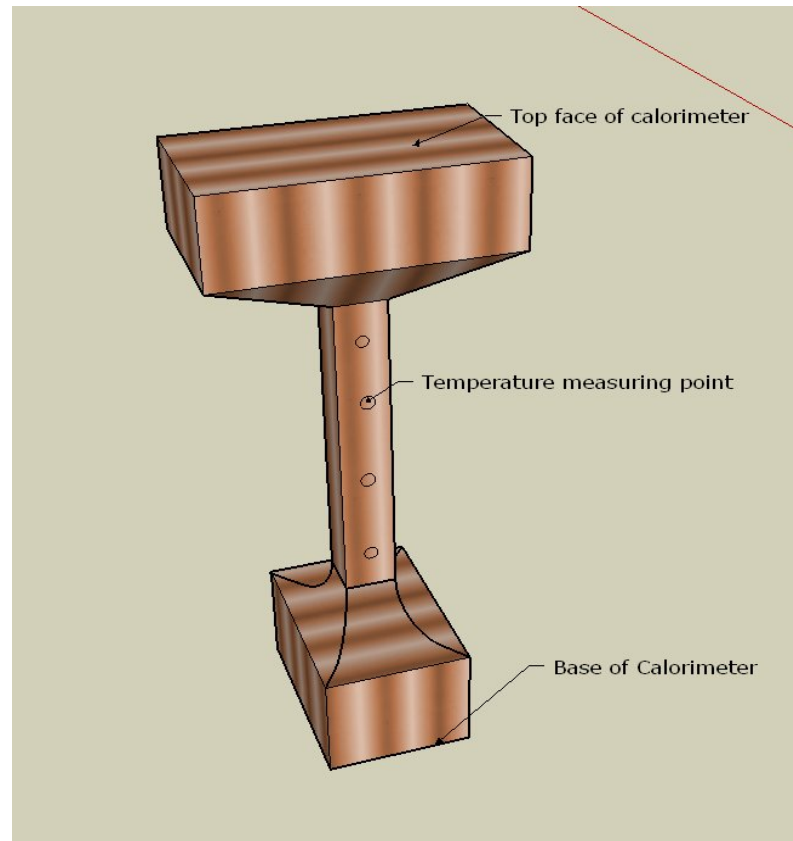


Figure 26: 3-D model of the Calorimeter used in final test setup (without the insulation cover).



## Calorimeter Insulation

The insulation cover was made from two separate rectangular slabs of insulating material which when held together formed a closed box like structure. A cavity, matching the profile of the calorimeter was engraved on the inner faces of the two slabs. This was done such that the whole of the calorimeter, along with the mounted MHP, could fit into the insulation cover box. The gaps, if any, between the calorimeter and the insulation covering, were manually filled with the same insulating material as that of the box. Figure 27 shows the calorimeter inside its insulation cover.

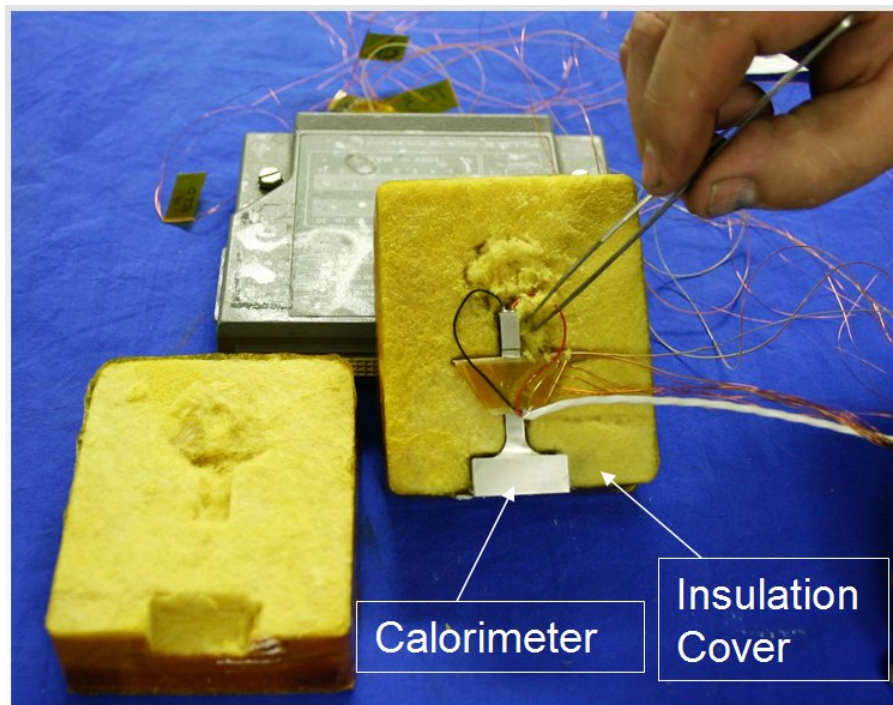


Figure 27: Calorimeter with the insulation cover.

## The Test Parameters

The temperature was measured at both ends of the MHP, the evaporator and the condenser end. OMEGA precision fine wire K-type thermocouples were used to measure the temperature. The temperature of the cold plate, which was cooled by circulating a mixture of water and ethylene glycol, was measured and held constant for a particular experiment. A Fischer-Scientific ISOTEMP 1013D, a controlled bath, was used to maintain the cooling mixture at the required temperature.

The power input to the heating element of the MHP was measured as the product of the voltage and current. A SPERRY DM-5300 digital multimeter was used to measure the voltage drop and the current was measured using an a/c clamp meter. The temperatures at the two ends of the die containing the MHP array and the four specified points along the height of the calorimeter were measured using the two K-type thermocouples mounted on the MHP lid and the four K-type thermocouples mounted on the calorimeter column respectively. A AGILENT 34970A data acquisition system was used to store the data.

## Charging and Sealing of the MHPs

Prior to the charging of the MHP array dies, the indium coated lids were thoroughly cleaned of oxides by immersing them in a dilute solution of hydrochloric acid and water (1:5) for about twenty seconds.

Then they were rinsed with acetone and allowed to dry. The die bases containing the 22 micro-channels were also cleaned by using the BRANSON solution which is a formulated cleaning concentrate. The MHP die bases were dipped into the solution for about two minutes and then rinsed with acetone and allowed to dry. Precautions were taken, so as not to touch the lids and die base with bare hands. This was done to avoid contaminating and damaging the micro structure.

Indium cold welding techniques are usually used in the macro world when, two sufficiently thick, clean indium-coated surfaces are brought into contact at room temperature and held together by applying some pressure. This is how the indium cold welding takes place [30]. As indium does not readily react with mercury, the above mentioned method was assumed safe for our experiment and was used in sealing the MHPs. For this purpose, one of the surfaces was deposited with a 1  $\mu\text{m}$  thick indium layer using an e-beam deposition machine during micro fabrication. The other surface was plated with a 10  $\mu\text{m}$  thick indium thereby providing sufficiently thick layers of indium on both the surfaces for bonding, as is required by the indium cold welding

process. After the cleaning of the lids and the bases of the MHPs, the bases of the die were manually charged/filled with the desired working fluid.

The charging of the MHPs was done using micro pipettes specially manufactured for this purpose. The lids were then placed on the die and the assembly was held together using mechanical clips.

In order to remove the non-condensable gases from the remaining volume of the micro heat pipes, the clipped assembly was then placed in a vacuum chamber. The arrangement was made such that, while the clipped dies were place in the vacuum chamber, the pressure exerted by the clips holding the lid and the base of the die together, increased slowly from initial pressure, which was just enough to hold the two parts together, to the final pressure which actually pressed them firmly together.

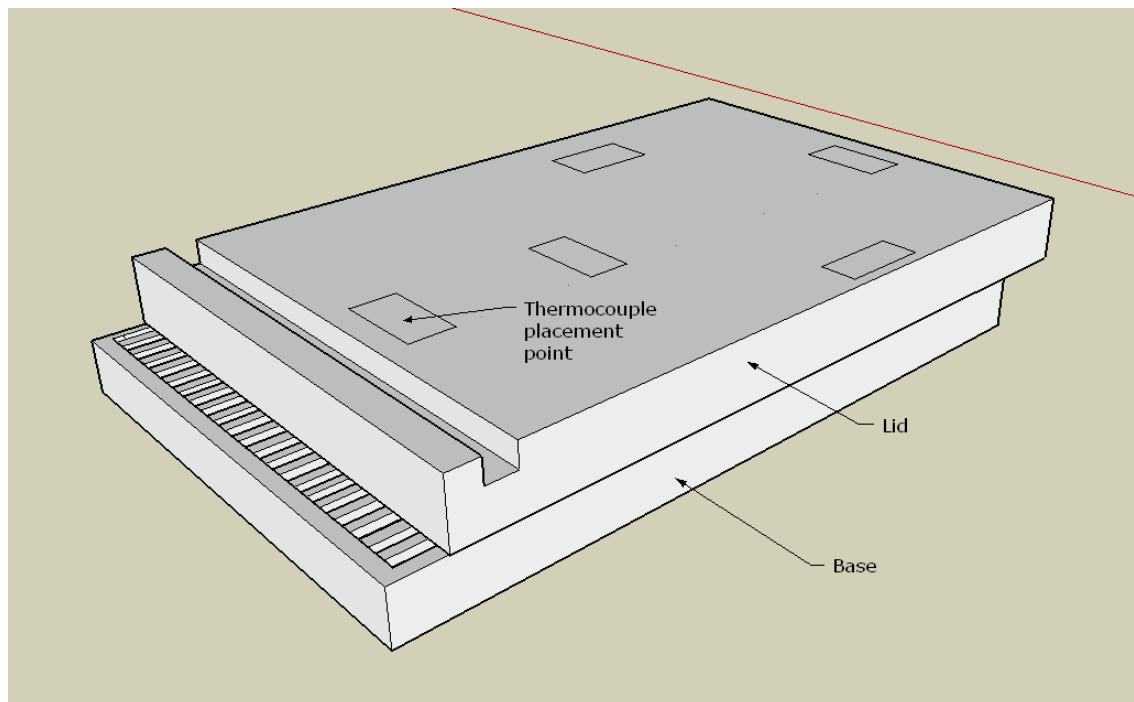


Figure 28: MHP array die and its components---lid and the base.

Thus, the non-condensable gases were allowed to escape from the clipped assembly of the MHP, while it was placed in the vacuum chamber for more than 24 hours at  $10^{-3}$  torr and at room temperature. After removing the attached lid and base assembly from the vacuum chamber, it was placed in the oven at an elevated temperature of 120 °C for the permanent sealing of the MHP. In Figure 28, the assembly of the MHP with its basic components viz; the base containing the micro channels and the lid with the groove for the placement of the heating element is shown.

### Test Procedure

The sealed MHP, with its heating element (in the groove on the lid) and the two temperature sensing thermocouples in their respective places, was placed on to the top face of the calorimeter. Silver based thermal grease, ELGR 8501, by AI Technology, was used to make good thermal contact between the lower face of the MHP containing die and the top face of the calorimeter. Then the calorimeter was placed on the cold plate and the same thermal grease was used to make thermal contact between the base of the calorimeter and the cold plate top face.

The insulation cover was then placed around the whole assembly. The multimeter and the ammeter were connected to the test setup. To start the experiment, the temperature of the fluid in the constant temperature bath, which was used as the cooling fluid in the cold plate, was set at the required point.

Upon reaching the set temperature, it was held constant throughout the duration of the experiment. Once the temperature of the cooling fluid in the constant temperature bath had reached the set point, the setup was ready and testing began.

Prior to the passing of any current through the heating element, readings for the temperatures at six different points were noted and recorded as zero input power readings. Out of the six temperature readings taken for every input power reading, one was noted at the evaporator end, one at the condenser end and the remaining four along the height of the calorimeter, at the previously described four temperature measuring points.

It was observed that for the zero input power readings, the temperature readings at the condenser end and evaporator end of the MHP were identical, indicating that the temperature throughout the heat pipe array was the same. To record the first set of readings, the Variac was adjusted to allow a small current, in the range of 0.25 to 0.50 A, to pass through the heating element. The heating of the tungsten element was clearly noticed, as the temperature measured by the thermocouple located above the evaporator end increased almost immediately. The six temperature readings were allowed to stabilize and then were recorded. The power was calculated as the product of the current and voltage drop, across the heating element. Thus, the first set of readings was completed.

For the next set of readings, the variac was re-adjusted to allow more current, of the order of few amperes, to pass through the heating element, and the same procedure as explained above was followed. Sufficient time intervals were maintained between the two consecutive readings to allow the MHPs to reach steady state operation.

## Performance Testing Parameters

The research work carried out on the MHPs can broadly be classified into two types viz: the theoretical work and the experimental work. Depending upon the type of research work undertaken, the parameters used to measure the performance of the MHP change.

Most of the theoretical work consists of the proposing of a mathematical model for the given test specimen, taking into account the various parameters such as substrate-working fluid combination, working temperature, orientation of MHP, dimensions of the MHP etc, and then verifying the mathematical model with the help of numerical simulation.

Sometimes there are certain constraints which cannot be incorporated into the model exactly as they are and therefore, need some modifications. These modifications can be in the form of boundary conditions or limits of integration. On doing so, they make the working of the mathematical model feasible. The assumptions thus made, sometimes may not accurately represent the exact actual working conditions.

These factors may be reflected in the fact that the parameters used to evaluate the performance of the MHPs are different for different research works. Thus, the comparison of the performance of various works is not easy.

C. B. Sobhan, R. L. Rag, and G. P. Peterson mention that, while theoretical studies focused on the variations of temperature and pressure of the working fluid inside the channels as the primary parameters, experimental studies have been directed at determination of the overall performance of the device through heat transfer and external

temperature measurements [14]. The same authors [14] have noted the different ‘performance indicators’. Effective thermal conductivity is one of the parameters which has been used to measure the performance. It is useful in comparing micro heat pipe performance when the channel arrangement is in longitudinal arrays.

Since the temperature drop in efficient micro heat pipes is normally very small, the effective conductivity values are very large [14]. Sometimes the thermal conductance or thermal resistances of the heat pipes are used as performance indicators. Comparison in terms of the heat transport per unit area of cross-section is a more direct method.

When various geometric designs for the cross-section are used, the heat transport per unit area of cross section is an effective method of comparing the micro heat pipes. This is so because the quantity per unit area remains independent of the number of channels used [14].

### Results from the Tests Conducted

Tests were conducted in the Auburn Thermo-Fluids Micro Measurement Laboratory (AuTherMML) on three types of MHPs. As mentioned earlier, the first type of MHP array was an empty MHP (vacuum sealed), the second was filled with water as the working fluid and the third was filled with mercury. All the tests were performed using the same test setup and under similar conditions so as to minimize the measurement errors.



Two specimens of mercury filled MHP, one specimen of water filled MHP and one empty MHP were tested. Following is the graph (Figure 29) showing the variation of the difference in the evaporator temperature and the condenser temperature for various power inputs. The graph contains the data collected from all the tests conducted on the empty MHP, the water filled MHP and the mercury filled MHP.

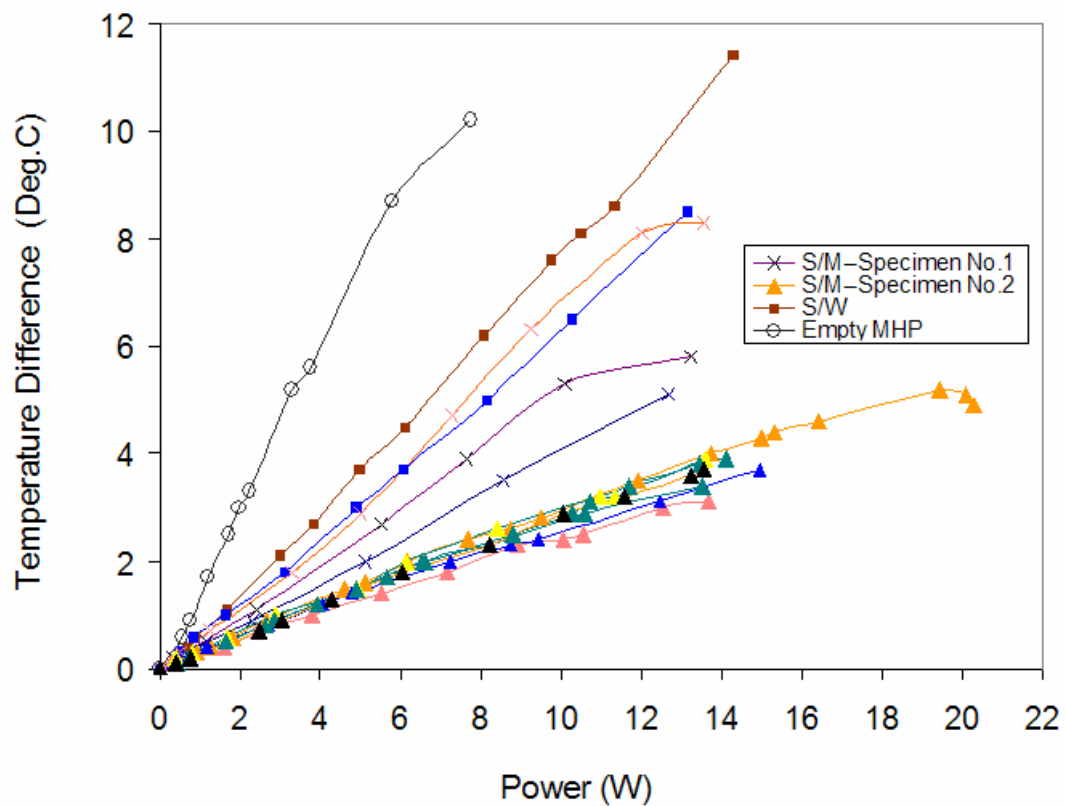


Figure 29: Graph showing the variations of the temperature difference between evaporator and condenser, with respect to power input, for various tests conducted.

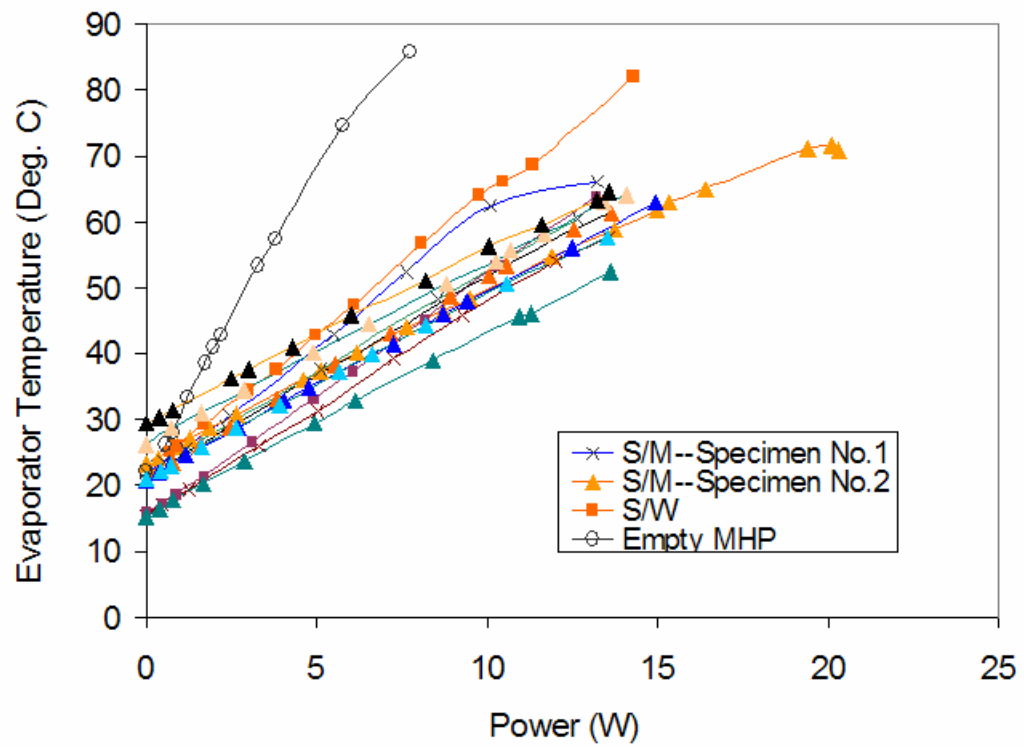


Figure 30: Graph showing the variation of the evaporator temperature with change in the power input.

It can be seen that the data for the different tests conducted on mercury filled MHPs are fairly consistent in their linear nature and are grouped close together. The tests were conducted on different occasions on the MHPs under similar testing conditions. The only change made in the testing conditions was that the set point for the cooling water bath temperature was varied for different test runs.

In some tests runs, the cooling water temperature was maintained close to room temperature, in some tests it was considerably lower (about 10 °C) than the room temperature while in some it was maintained above room temperature.

This change in the testing condition is clearly reflected in the graph shown in Figure 30 which plots the variation of evaporator temperature against the various input powers. It can be observed that some of the test runs show the initial evaporator temperature (for 0 W input) close to room temperature (which was usually around 23 °C to 24 °C), some well below that temperature mark (at about 15 °C) and some distinctly above the room temperature mark (at about 27 °C to 30 °C).

In the published paper “The performance of micro heat pipes measured by integrated sensors”, a correlation between the heat sink temperature and the effective thermal conductivity was reported by Martine Le Berre *et al.* In their work, they have stated that—“we observe that the equivalent thermal conductivity ‘K<sub>eff</sub>’ increases with the cooling temperature” [5].

Seok Hwan Moon *et al.* have mentioned in their work, the testing of the MHP with the temperature at the condenser end lower by 5 °C to 20 °C than that of the surrounding or room temperature.

They reported a decrease in the heat transfer rate of the MHP in such a case and attributed the result to the ‘liquid blocking’. Liquid blocking region is defined as the region created at the condenser end, where the vapor could not be reached and the heat transfer by phase change cannot be accomplished [15].

Two methods were adopted to calculate the values for the thermal conductivity, which is one of the important ‘performance testing parameters’. The first method used was more of an indirect method as it was based on comparison and the second was a direct method which used a modified form of the Fourier’s law to calculate the values for thermal conductivity.

For the first method, the slope of the graph for the variation of the temperature difference, between the evaporator and the condenser end, plotted against the power input was calculated (Figure 29). The slope is the value of the ratio of temperature difference to the input power. Silicon equivalence for a particular MHP was then calculated as the ratio of the slope of the empty MHP to the slope of the required MHP. Finally, the silicon equivalence was multiplied by the known value for the thermal conductivity of silicon, to obtain the equivalent thermal conductivity of that particular MHP. Table 5 shows the calculations for the above explained procedure.

**Calculation of Equivalent Thermal Conductivity Using the Silicon Equivalence Approach**

K silicon (W/m-K)	Name	Equation	Slope ( $\Delta T/\Delta Q$ )	R <sup>2</sup> Value	Silicon Equivalence	Equi. Thermal cond.(W/m-K)
148	Empty MHP	1.3968x+0.1111	1.397	0.9882	1	148.0
	S/W-1	0.793x-0.2012	0.793	0.9987	1.76	260.7
	S/W-2	0.638x-0.0643	0.638	0.9987	2.19	324.0
	S/M-1	0.4689x+0.0895	0.469	0.9836	2.98	440.9
	S/M-2	0.4009x+0.0214	0.401	0.9993	3.48	515.7
	S/M-3	0.6525x-0.105	0.653	0.993	2.14	316.8
	S/M-4	0.2329x+0.0678	0.233	0.9956	6.00	887.6
	S/M-5	0.246x+0.1009	0.246	0.9954	5.68	840.4
	S/M-6	0.2618x+0.0882	0.262	0.9898	5.34	789.6
	S/M-7	0.2824x+0.1128	0.282	0.9963	4.95	732.0
	S/M-8	0.2797x+0.0614	0.280	0.9978	4.99	739.1
	S/M-9	0.2742x+0.0413	0.274	0.9978	5.09	753.9
	S/M-10	0.259x+0.2169	0.259	0.9861	5.39	798.2

Table 5: Equivalent thermal conductivity calculation, based on silicon equivalence approach. (S/W =silicon/water,  
S/M=silicon/mercury)

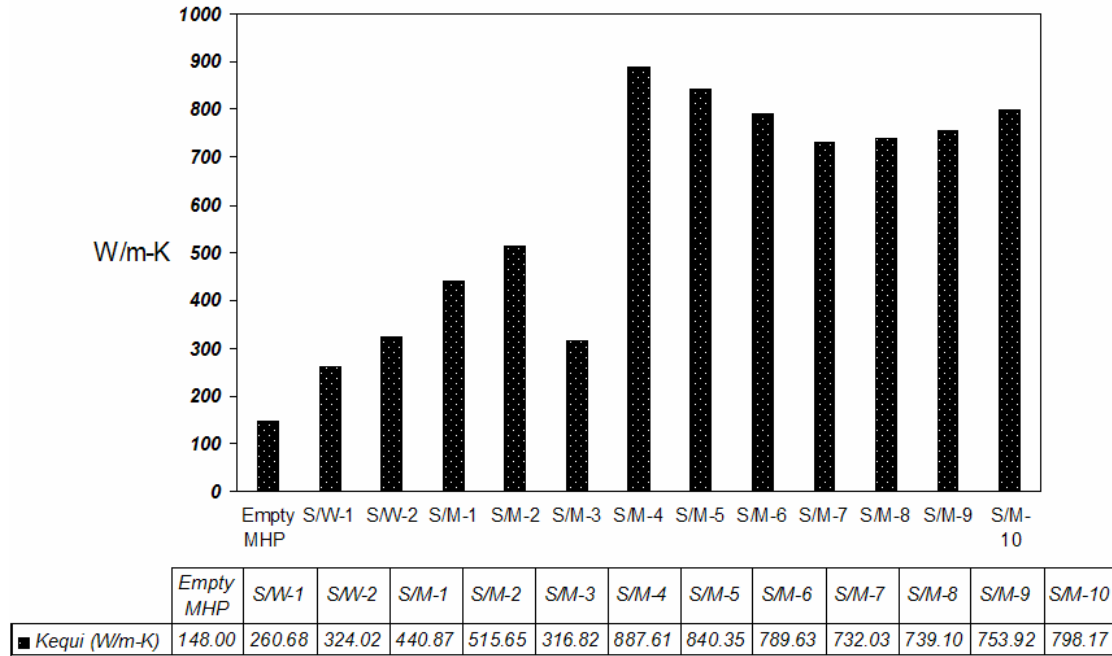


Figure 31: Graph showing the variation of equivalent thermal conductivity, calculated using silicon equivalence method versus input power. (S/W=silicon/water and S/M=silicon/mercury).

The second approach used to calculate the thermal conductivity of the MHP was that of the effective thermal conductivity. In this method, the values for the effective thermal conductivity for each MHP were calculated independently. Thus, there was no dependence on the value of the thermal conductivity of the empty MHP.

Effective thermal conductivity ( $K_{eff}$ ) is one of the important parameters of comparison for the MHPs. Values were calculated using the modified Fourier's law as follows.

$$K_{eff} = [(Q / Amhp)] / [(T_{max} - T_{min}) / L] \quad (4.1)$$

where,  $Q$  = Input power,

$L$  = Length of the MHP,

$A_{mhp}$  = Area of the MHP array,

$T_{max}$  = Temperature at evaporator end for given  $Q$ ,

$T_{min}$  = Temperature at condenser end for given  $Q$ .

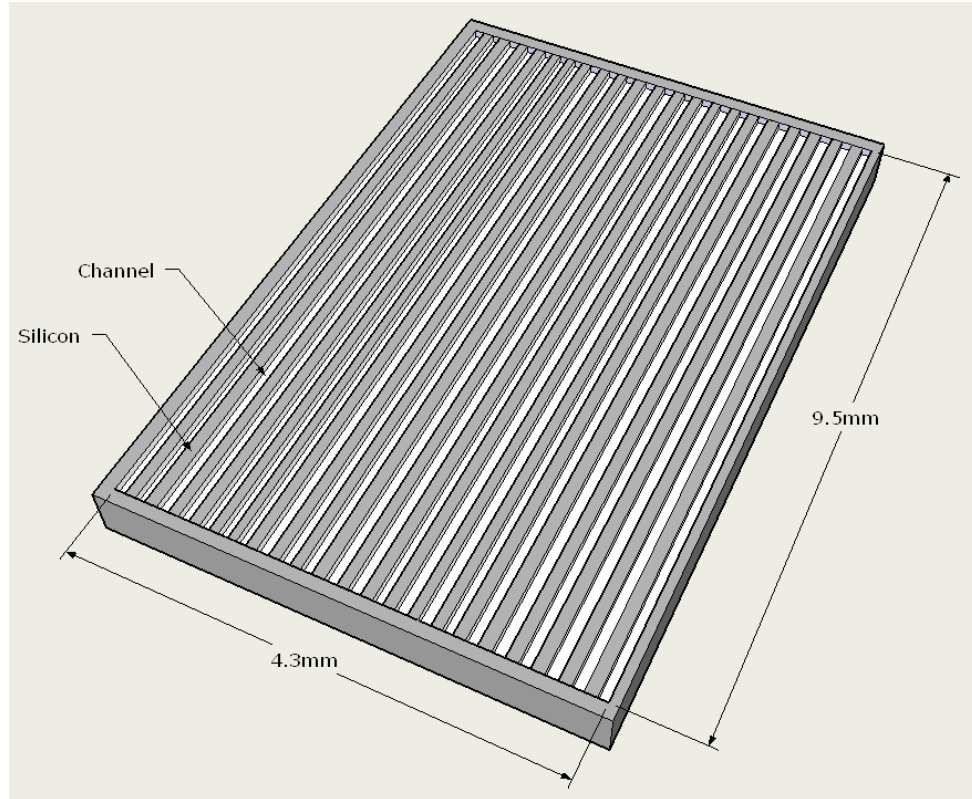


Figure 32: MHP base dimensions.

The area of the MHP array was considered to be equal to the total area occupied by the 22 channels and the 21 silicon rows between these channels. It was calculated as the sum of the products of the length and the width of each MHP.

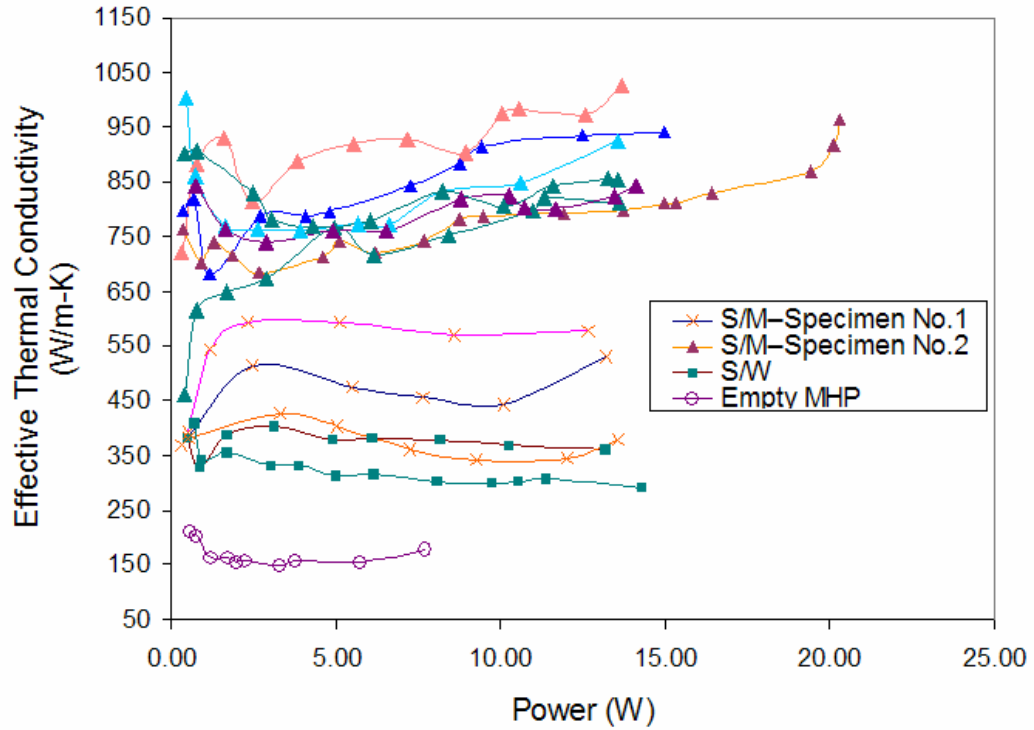


Figure 33: Comparison of the effective thermal conductivity versus input power, for various MHPs.

As expected, the water filled MHP had its effective thermal conductivity lower than that of the mercury filled MHP and higher than that of the empty MHP. Also, it was observed that the readings for the empty MHP had the effective thermal conductivity in the range of 153 W/m-K to 208 W/m-K with the average value being 167.5 W/m-k and the average thermal resistance being 1.40 °C/W. For the major part of the experiment, the empty MHP exhibited the thermal conductivity in the range of 150 W/m-K which was in close proximity to the commonly referred value for silicon thermal conductivity [4, 31, 32]. Thus, it was seen that the experimental value for the empty MHP, was in close agreement with the theoretical value available in the literature.



The two specimens of mercury filled MHP which were tested differed from each other only in terms of their charge. Apart from this difference both the MHPs were the same in all other respects, such as their dimensions and material of construction. The second specimen was filled with less charge than the first one and there was a noticeable difference in the recorded thermal conductivities of the two specimens. The MHP with the lesser charge exhibited better performance. Since, with the given apparatus, it was not possible to measure the exact amount of the charge being filled in the MHP, no such quantitative measurements were made. The charge of two mercury filled MHPs, was compared on the basis of visual inspection done at the time of charging of the MHPs. The results for effective thermal conductivity of MHPs are plotted in Figure 33. Another important parameter of measurement of the performance of the MHP is their thermal resistance. The thermal resistance values were calculated using the following formula.

$$\text{Thermal Resistance} = \Delta T / \text{Power} \quad (4.2)$$

where,  $\Delta T$  = Temperature difference between the evaporator and  
condenser regions of the MHP.

Power = Input power to the MHP.

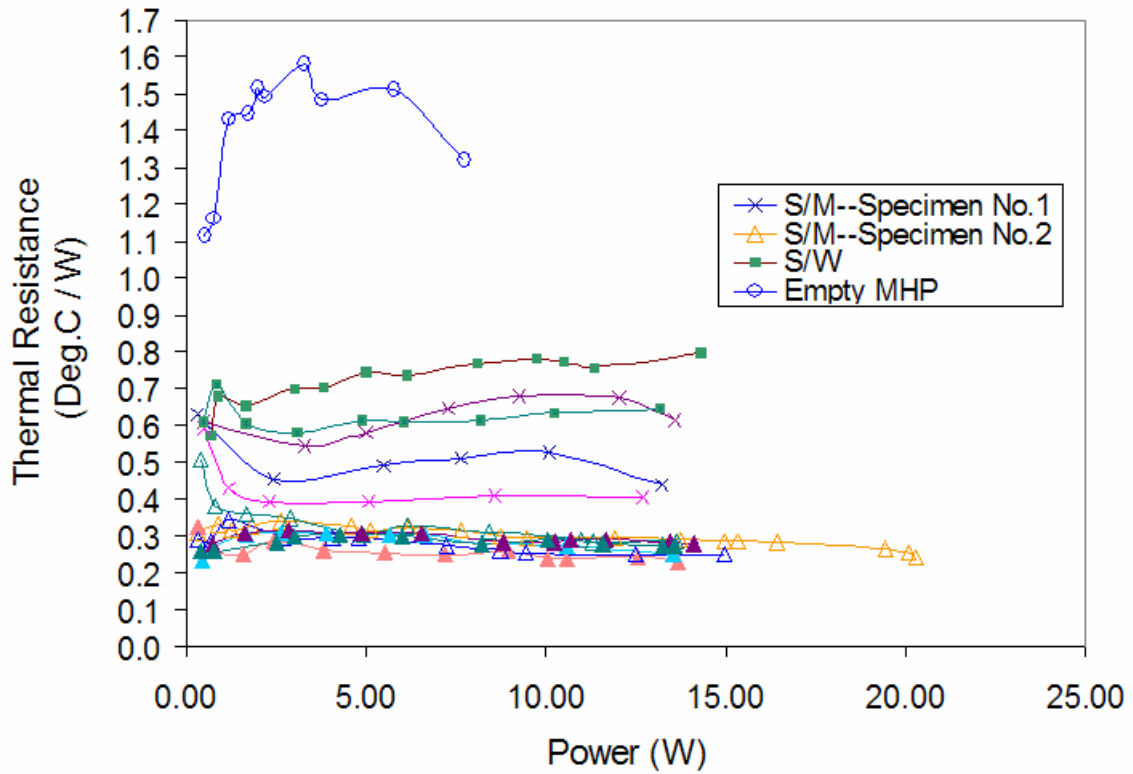


Figure 34: Thermal resistance vs. the input power for various MHPs.

The thermal resistance for the mercury filled MHPs was comparatively high at the initial power inputs which were low (start up condition), and had a tendency to decrease further as the power input increased. This behavior could be interpreted as the improvement in the performance of the MHP with an increase in the working temperature or increase in the power input. Also, it was observed that the mercury filled specimen no. 2 showed very close results for all the test runs.

High heat fluxes were recorded with the testing of the liquid metal filled MHPs. Table 6 lists the recorded values of heat fluxes for the three types of MHPs. As seen in Table 6, the highest value of heat flux was recorded with the mercury filled MHP. However, the value of  $49.69 \text{ W/cm}^2$  was not the higher limit of the working MHP. It was the limitation of the tungsten coil used as the heating element which either burnt out at higher power values or lost electrical contact with the lead wires. Due to this reason, the higher heat fluxes could not be achieved during the testing.

	Empty MHP	S/W--1	S/M--10
Power (W)	7.74	14.30	20.30
Tmax (Evaporator) °C	85.7	82	70.8
$\Delta T$	10.2	11.4	4.9
Maximum Flux (W/cm <sup>2</sup> )	18.94	35.01	49.69
Maximum Flux (W/m <sup>2</sup> )	1.89E+05	3.50E+05	4.97E+05

Table 6: Comparison of the heat flux through MHP (S/W= Silicon/Water, S/M=Silicon/Mercury).

The following figures compare the performances of all the MHPs tested at AuTherMML. The first graph, Figure 35, plots the average ‘Keff’ of the various MHPs. The second comparison is based on the enhancement factor, Figure 36, which measures how well the other MHPs performed, considering the performance of the empty MHP as the datum. The enhancement factor was defined as the ratio of the average effective thermal conductivity of a given MHP to the average effective thermal conductivity of the empty MHP.

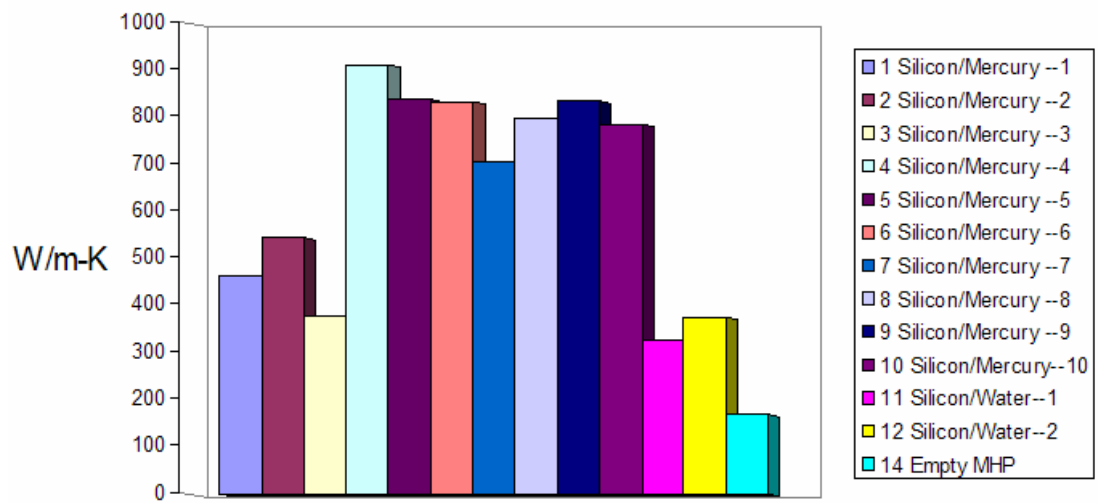


Figure 35: Comparison of various MHPs using the average effective thermal conductivity.

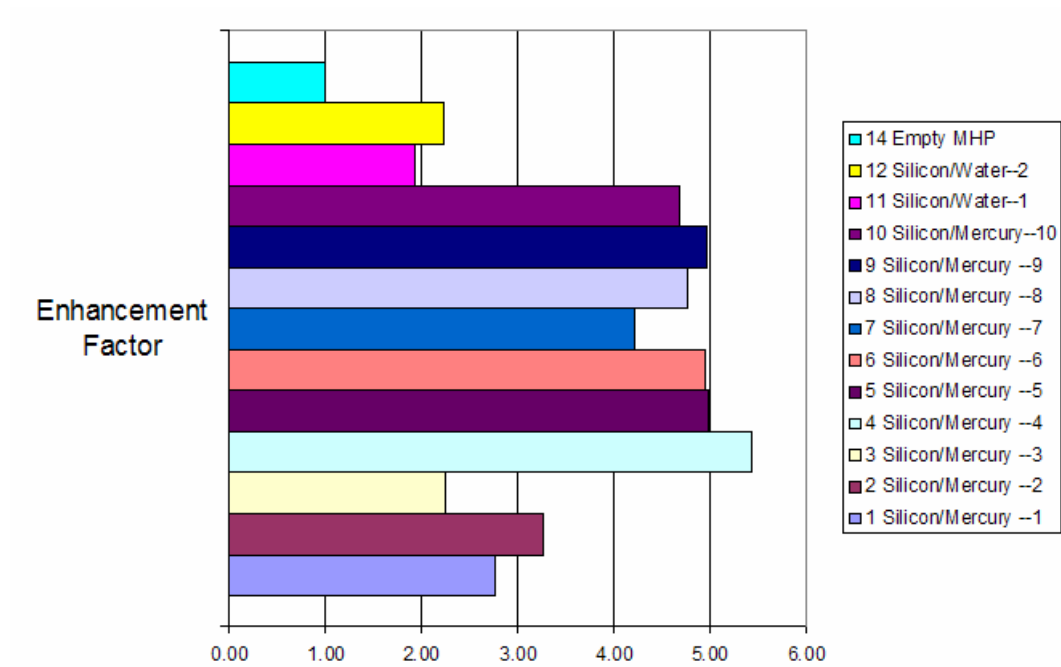


Figure 36: Comparison of various MHPs in terms of improvement of ‘Keff’ over the empty MHP (enhancement factor).

The two methods used to evaluate the thermal conductivities of the MHPs have been graphically compared in Figure 37. Most of the tests conducted, show similar values using both the methods viz. the equivalent thermal conductivity and the effective thermal conductivity method. Figure 38 gives a size comparison between the MHP array die and a coin. Figure 39 shows the final test setup used for testing.

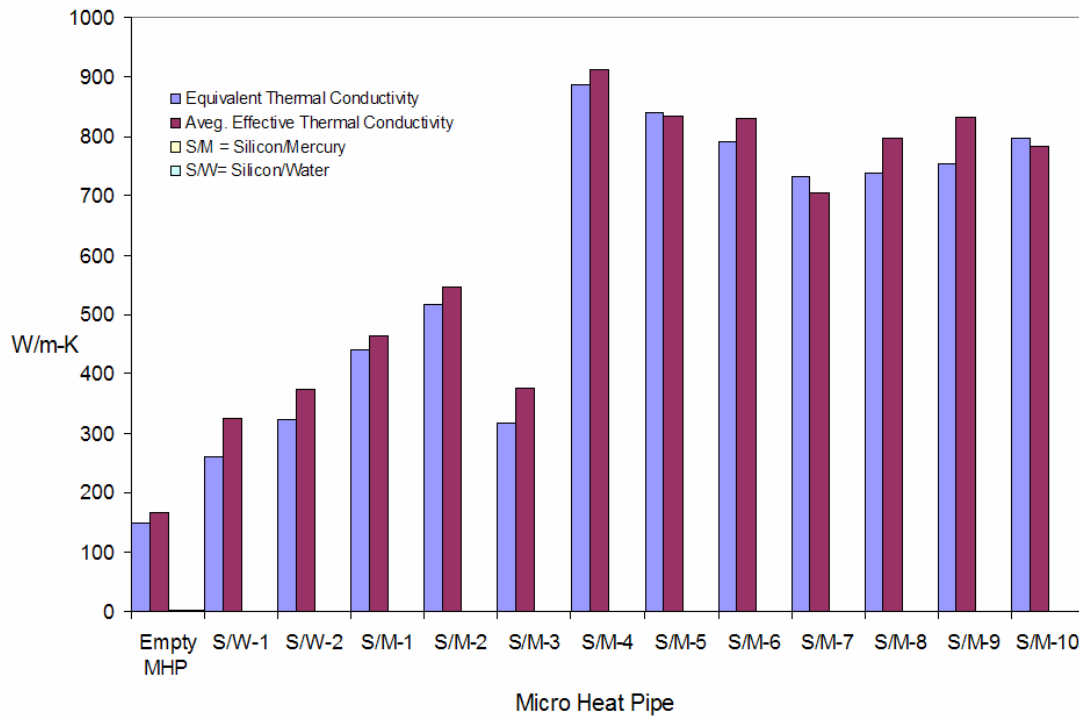


Figure 37: Comparison of the results from the two methods used to calculate the thermal conductivity.

TABLE 144. Recommended thermal conductivity of silicon†  
(Temperature,  $T$ , K; Thermal Conductivity,  $k$ , W cm<sup>-1</sup> K<sup>-1</sup>)

Solid			
$T$	$k$	$T$	$k$
0	0	250	1.91
1	0.0693*	273.2	1.68
2	0.454	298.2	1.49
3	1.38	300	1.48
4	2.97	323.2	1.33
5	5.27	350	1.19
6	8.23	373.2	1.08
7	11.7	400	0.989
8	15.5	473.2	0.814
9	19.5	500	0.762
10	23.3	573.2	0.651
11	27.0	600	0.619
12	30.9	673.2	0.536
13	34.8	700	0.508
14	38.4	773.2	0.442
15	41.6	800	0.422
16	44.1	873.2	0.374
18	47.7	900	0.359
20	49.8	973.2	0.323
25	51.3	1000	0.312
30	48.1	1073.2	0.286
35	41.3	1100	0.279
40	35.3	1173.2	0.262
45	30.6	1200	0.257
50	26.8	1273.2	0.247
60	21.1	1300	0.244
70	16.8	1373.2	0.237
80	13.4	1400	0.235
90	10.8	1473.2	0.229
100	8.84	1500	0.227
123.2	5.99	1573.2	0.223
150	4.09	1600	0.221
173.2	3.30	1673.2	0.220
200	2.64	1685	0.220
223.2	2.25		

†The values are for well-annealed high-purity silicon, and those below room temperature are merely typical values.

\*Extrapolated.

Table 7: Silicon thermal conductivity [32].

TABLE 96. Recommended thermal conductivity of mercury†  
(Temperature,  $T$ , K; Thermal Conductivity,  $k$ , W cm<sup>-1</sup> K<sup>-1</sup>)

Solid				Liquid	
	to triagonal axis	⊥ to triagonal axis	Poly- crystal- line		
$T$	$k$	$k$	$k$	$T$	$k$
0	0	0	0	234.288	0.0697
1	82.4*	57.2*	65.6*	250	0.0732
2	21.5*	14.9*	17.1	273.2	0.0782
3	6.34*	4.40*	5.05	298.2	0.0830
4	2.84*	1.97*	2.26*	300	0.0834
5	1.66*	1.15*	1.32*	323.2	0.0874
6	1.11*	0.770*	0.882*	350	0.0915
7	0.834*	0.581*	0.665*	373.2	0.0947
8	0.691*	0.481*	0.551*	400	0.0984
9	0.615*	0.429*	0.491*	473.2	0.107
10	0.576*	0.400*	0.460*	500	0.110
11	0.559*	0.387*	0.445*	573.2	0.117
12	0.547*	0.382*	0.437*	600	0.120
13	0.538*	0.377*	0.432*	673.2	0.126
14	0.532*	0.373*	0.427*	700	0.127
15	0.527*	0.369*	0.422*	770	0.1283
16	0.522*	0.366*	0.418*	773	0.128
18	0.512*	0.360*	0.410*	800	0.128
20	0.504*	0.354*	0.404*	873.2	0.126
25	0.488*	0.343*	0.392*	900	0.124*
30	0.474*	0.334*	0.382*	973.2	0.119*
35	0.462*	0.327*	0.373*	1000	0.117*
40	0.452*	0.320*	0.365*	1073.2	0.111*
45	0.444*	0.315*	0.359*	1100	0.108*
50	0.437*	0.311*	0.354*	1173.2	0.101*
60	0.424*	0.304*	0.345*	1200	0.0984*
70	0.413*	0.297*	0.337*	1273.2	0.0904*
80	0.404	0.293	0.330*	1300	0.0872*
90	0.396	0.288	0.324	1373.2	0.0773*
100	0.390	0.285	0.320	1400	0.0732*
123.2	0.374	0.279	0.310	1473.2	0.0610*
150	0.360	0.271	0.301	1500	0.0559*
173.2	0.349	0.268	0.295	1573.2	0.0407*
200	0.340	0.264	0.289	1600	0.0345*
223.2	0.332	0.260	0.285	1673.2	0.0164*
234.288	0.329	0.259	0.282	1700	0.0094*
				1733	0.00045*

†The values are for high-purity mercury. Those for liquid mercury above 1000 K are provisional and those for solid mercury below 80 K are merely typical values.

\*Extrapolated or estimated.

Table 8: Mercury thermal conductivity [32].



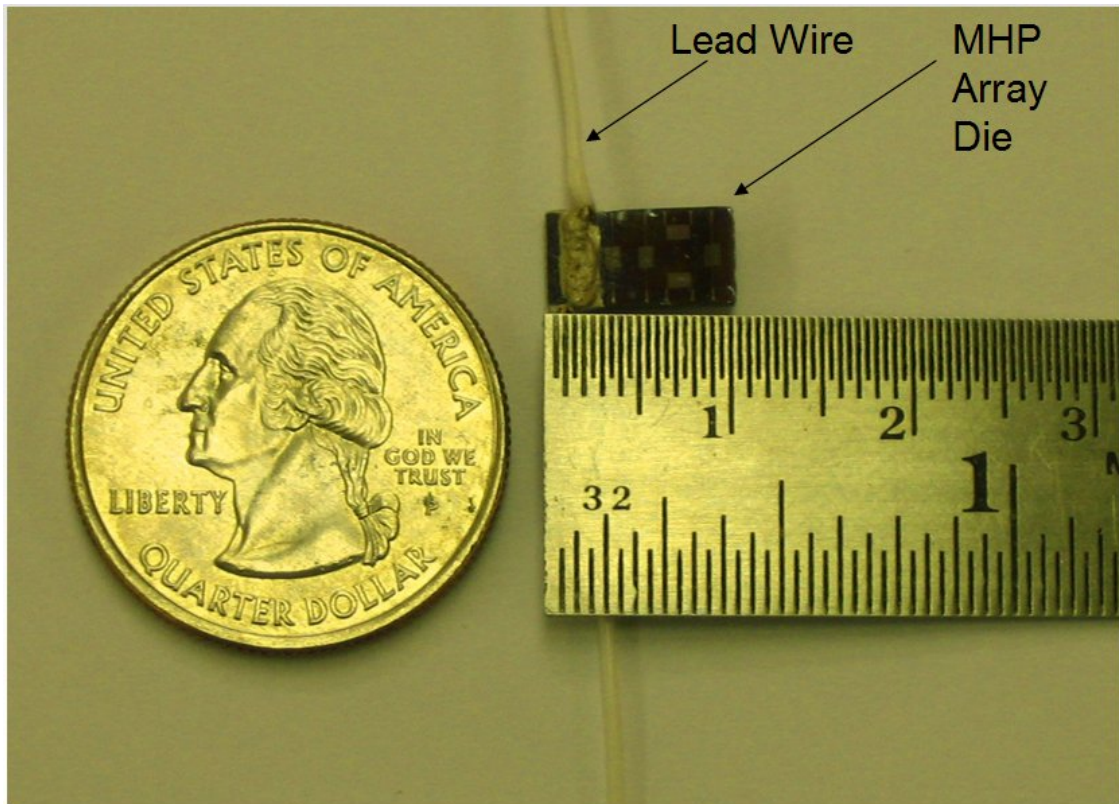


Figure 38: Actual MHP size comparison.

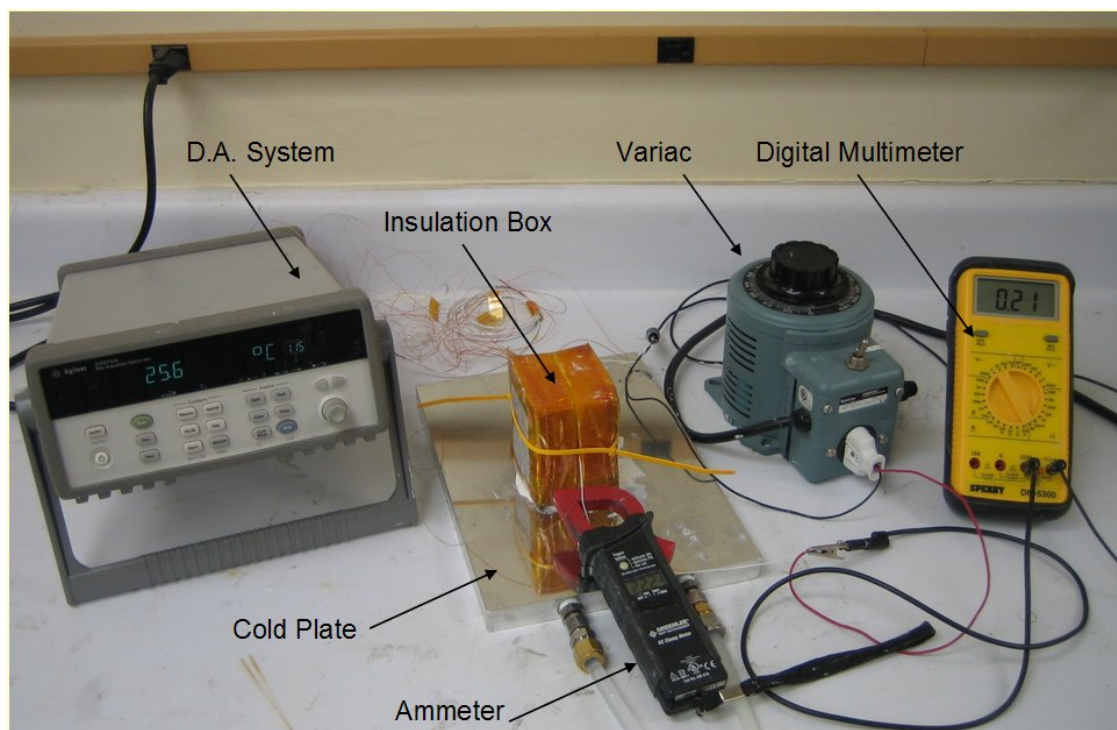


Figure 39: Test setup.

## CHAPTER 5

### UNCERTAINTY ANALYSIS

The exact measurement of the parameters which determine the performance of a particular experiment cannot be done. Therefore it is preferable to perform an uncertainty analysis. This analysis helped in predicting the uncertainty of the recorded or measured values with regard to the actual (unknown) values.

Errors are introduced into the experiment on account of various factors. Some of these factors are human error, errors present in the measuring instrument, the errors introduced due to the experimental setup etc. It is practically impossible to eliminate all the errors and get the exact results from the experiment. Thus, an attempt is made to first identify the errors and then minimize their magnitude. Uncertainty of a measured value is an interval around that value such that any repetition of the measurement will produce a new result that lies within this interval. This uncertainty interval is assigned by the experimenter following the established principles of uncertainty estimation.

In the tests performed on the MHPs, the input variables such as the voltage and current to the heating element of the MHP were measured and the resultant changes in temperature along the axial length of the MHP were recorded.

These values along with the other known values such as the dimensions of the MHP were then used to calculate the effective thermal conductivity of the MHP. An analysis was carried out so as to find out the uncertainty in the calculated effective thermal conductivity.

The values for the accuracy of the multimeter and the ac clamp meter, used to measure the voltage and the current respectively, were obtained from the instruction manuals provided by the manufacturer. Also, the error in the K-type thermocouples, used to measure the temperatures at the evaporator and condenser ends, were noted from the specifications as published by the manufacturer. The possible human error in the placement of the thermocouples was also included in the uncertainty analysis. The formulae used to calculate the power and Keff include the mathematical operations of product and quotient being performed on the measured and known values of parameters mentioned above. Thus, the uncertainty in the calculated values of power and the thermal conductivity can be determined by using the following approach.

If ‘A’ is the quantity of our interest and, if it depends on a number of variables  $x, \dots, z$  and  $u, \dots, w$  in the relation given by formula (5.1)

$$A = (x * \dots * z) / (u * \dots * w) \quad (5.1)$$

then, the fractional uncertainty in A,  $(\partial A/A)$ , is given by formula (5.2)

$$(\partial A/|A|) = \sqrt{(\partial x/|x|)^2 \dots + \dots (\partial z/|z|)^2 + (\partial u/|u|)^2 \dots + \dots (\partial w/|w|)^2} \quad (5.2)$$

Where,  $\partial x$ ,  $\partial z$ ,  $\partial u$  and  $\partial w$  are the uncertainties with which the values of  $x$ ,  $z$ ,  $u$  and  $w$  are measured [33]. The following example will clarify the method used to calculate the uncertainties in the current work. The measurements are from the test conducted on the empty MHP. For a particular reading, the recorded values for the voltage and current were 1.4 V and 2.7 A respectively. The formula to calculate the accuracy of the voltmeter in the range of 20 V was given as  $\pm (0.012 \cdot \text{Reading} + 0.001)$ . Thus, the accuracy of the reading for 1.4 Volts was  $\pm (0.012 \cdot 1.4 + 0.001) = 0.0178$ , which was rounded off to the value of 0.02. The fractional uncertainty for voltage was calculated as the ratio of the accuracy of the voltmeter to the recorded value of voltage. Thus in this case, the fractional uncertainty was  $(0.02/1.4) = 0.01$ .

To calculate the accuracy for the reading of 2.7 Amperes the formula  $\pm (0.03 \cdot \text{Reading} + 0.05)$  was used, which was the formula provided by the manufacturer for the ac clamp meter, when used in the range of 19.99 A. The accuracy of the reading 2.7A was  $\pm (0.03 \cdot 2.7 + 0.05) = 0.131$ , which was rounded off to 0.13. The fractional uncertainty for amperes was calculated as the ratio of the accuracy for the ammeter to the actual value of recorded amperes. Thus, its value was  $(0.13/2.7) = 0.05$ .

The error in the readings for the thermocouples, used to measure the temperature, was obtained from the manufacturer's website. The error in placement of the thermocouples, at the required positions of evaporator and condenser, was assumed to be 0.0002 m. This value was obtained from the dimensions of the RTDs patterned on the top face of the lid, which acted as the thermocouple placement points.

The values for the fractional uncertainties in evaporator temperature, condenser temperature, the difference between these two temperatures and the fractional uncertainty in the placement of the thermocouples at their measurement points were calculated.

Once the fractional uncertainties for all the individual parameters such as current, voltage, temperature, temperature difference and the placement of thermocouples were calculated, the fractional uncertainty for the effective thermal conductivity ( $K_{eff}$ ) which depends on these parameters, was calculated using the above mentioned formula and its value was found to be 0.061. Then, to calculate the actual uncertainty in the value of ' $K_{eff}$ ', the fractional uncertainty in ' $K_{eff}$ ' was multiplied by the value of ' $K_{eff}$ '. The value for ' $K_{eff}$ ' was found using the modified Fourier's law  $K_{eff} = (Q / A) * (L / \Delta T)$  and was found to be 156.98 W/m-K for the particular case considered in this example. Thus, the value for the uncertainty in the value of ' $K_{eff}$ ' was the product of the calculated ' $K_{eff}$ ' and the fractional uncertainty given by  $(156.98 * 0.061) = 9.57$  with a 95% level of confidence. This value can be interpreted as follows. When the calculated value of the ' $K_{eff}$ ' is 156.98 W/m-K, its true value can lie anywhere in between the values  $156.98 \pm 9.57$ . The actual value of ' $K_{eff}$ ' can be thus considered to lie between 147.41 W/m-K and 166.55 W/m-K. A similar approach was used to find out the uncertainty in the power measured.

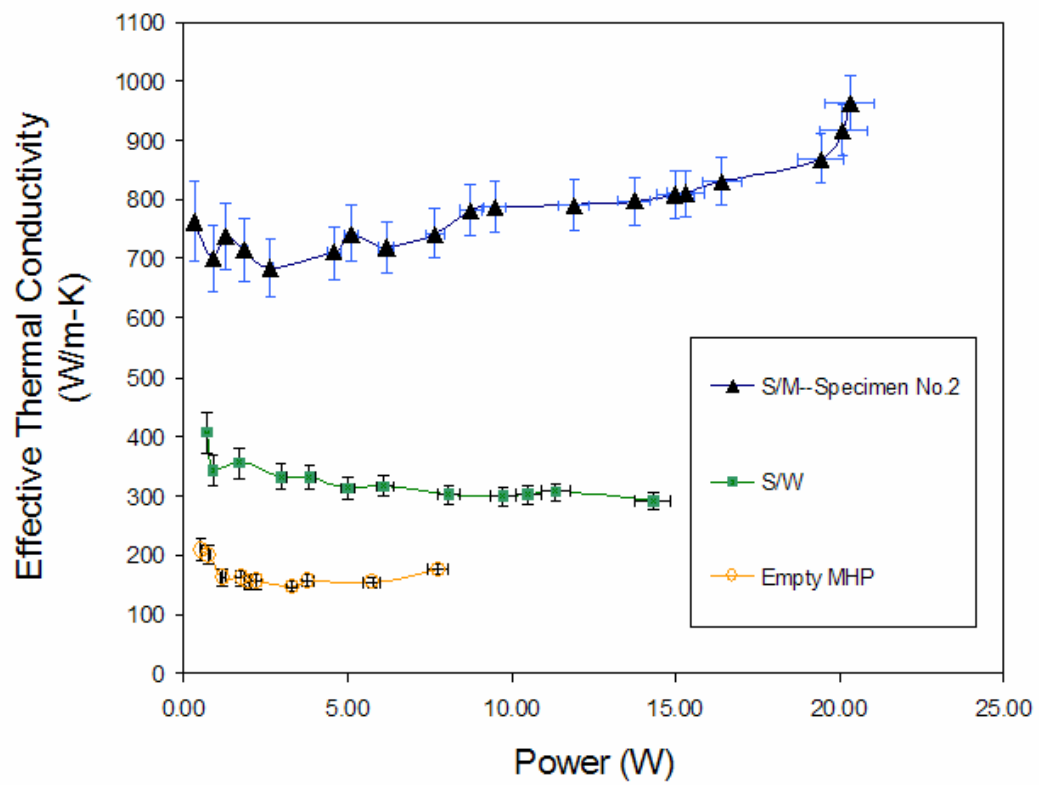


Figure 40: Uncertainty analysis performed on the three types of MHPs.

## CHAPTER 6

### DISCUSSIONS

#### Overview

In this work carried out at AuTherMML in Auburn University, three types of MHPs were tested. Two MHP specimens were charged with mercury, one with water and the third type was an empty MHP. The testing procedures and the test results were presented. In order to eliminate the systematic bias in the measurement of the thermal conductivity of the MHPs, the method of comparison using the silicon equivalence was used. The second method used the modified form of the Fourier's law to determine the thermal conductivity. It was observed that the two methods used to measure the thermal conductivities provided results in close agreement with each other for most of the test conducted. Silicon equivalence value of 6 was achieved and thermal conductivity as high as 900 W/m-k was reported for a MHP filled with mercury.



## Conclusion

The concept of liquid metal micro heat pipes was validated. This was the first time that a liquid metal micro heat pipe was completely manufactured and tested. As mentioned in one of the papers by P. Ramadas *et al.* [34] “liquid metal micro heat pipes have not been completely fabricated nor tested”. It was demonstrated through testing of these MHPs that the liquid metal filled MHPs perform better than the water filled MHPs.

## Future Work and Recommendations

It is proposed to replace mercury by gallium as the working fluid in the future liquid metal filled MHPs. This is due to the toxicity concerns related to the use of mercury. Gallium has been used by others for its conduction ability, but there are other issues related to the use of gallium. Gallium is reactive in nature and forms oxides very easily. It is also a rare element and is therefore quite expensive.

There are plans to scale-up the fabrication process for the MHPs. Currently the TRL (Technology Readiness Level) is about 2 and it is proposed to take up this level up to TRL 6 so as to facilitate the batch production of the MHPs.

Technology Readiness Levels (TRLs) are a systematic metric/measurement system that supports assessments of the maturity of a particular technology and the consistent comparison of maturity between different types of technology [35].

The method of charging the MHPs can be automated and an arrangement to measure the charge being filled can be made. The placement of the heating element in the groove on the MHP array die can be made easier with the inclusion of a supporting mechanism for the lead wires in the existing test setup.

## BIBLIOGRAPHY

- [1] G. P. Peterson, "Overview of micro heat pipe research and development," *Applied Mechanics Reviews*, vol. 45, pp. 175-189, 1992.
- [2] G. P. Peterson, *An Introduction to Heat Pipes--Modeling, testing and applications*: John Wiley & Sons, Inc., 1994.
- [3] P. D. Dunn and D. A. Reay, *Heat pipes*, 3rd ed. Oxford Oxfordshire ; New York: Pergamon Press, 1982.
- [4] B. Badran, F. M. Gerner, P. Ramadas, T. Henderson, and K. W. Baker, "Experimental results for low-temperature silicon micromachined micro heat pipe arrays using water and methanol as working fluids," *Experimental Heat Transfer*, vol. 10, pp. 253-272, 1997.
- [5] M. Le Berre, G. Pandraud, P. Morfouli, and M. Lallemand, "The performance of micro heat pipes measured by integrated sensors," *Journal of Micromechanics and Microengineering*, vol. 16, pp. 1047-1050, 2006.
- [6] G. P. Peterson, A. B. Duncan, A. S. Ahmed, A. K. Mallik, and M. H. Weichold, "Experimental investigation of micro heat pipes in silicon wafers," presented at Winter Annual Meeting of the American Society of Mechanical Engineers, Dec 1-6 1991, Atlanta, GA, USA, 1991

- [7] A. Lai, C. Gillot, M. Ivanova, Y. Avenas, C. Louis, C. Schaeffer, and E. Fournier, "Thermal characterization of flat silicon heat pipes," in Twentieth Annual IEEE Semiconductor Thermal Measurement and Management Symposium, 9-11 March 2004, Twentieth Annual IEEE Semiconductor Thermal Measurement and Management Symposium (IEEE Cat. No.04CH37545). San Jose, CA, USA: IEEE, 2004, pp. 21-5 BN - 0 7803 8363 X.
- [8] A. K. Mallik and G. P. Peterson, "Steady-state investigation of vapor deposited micro heat pipe arrays," *Journal of Electronic Packaging, Transactions of the ASME*, vol. 117, pp. 75-81, 1995.
- [9] M. Le Berre, S. Launay, V. Sartre, and M. Lallemand, "Fabrication and experimental investigation of silicon micro heat pipes for cooling electronics," *Journal of Micromechanics and Microengineering*, vol. 13, pp. 436-441, 2003.
- [10] D. Wu, G. P. Peterson, and W. S. Chang, "Transient experimental investigation of micro heat pipes," *Journal of Thermophysics and Heat Transfer*, vol. 5, pp. 539-544, 1991.
- [11] J. S. Park, J. H. Choi, H. C. Cho, S. S. Yang, and J. S. Yoo, "Flat micro heat pipe arrays for cooling and thermal management at the package level," presented at Design, Test, Integration, and Packaging of MEMS/MOEMS 2001, 25-27 April 2001 Proceedings of the SPIE - The International Society for Optical Engineering, Cannes, France, 2001.
- [12] S.-W. Kang, S.-H. Tsai, and H.-C. Chen, "Fabrication and test of radial grooved micro heat pipes," *Applied Thermal Engineering*, vol. 22, pp. 1559-1568, 2002.

- [13] M. Lee, M. Wong, and Y. Zohar, "Characterization of an integrated micro heat pipe," *Journal of Micromechanics and Microengineering*, vol. 13, pp. 58-64, 2003.
- [14] C. B. Sobhan, R. L. Rag, and G. P. Peterson, "A review and comparative study of the investigations on micro heat pipes," *INTERNATIONAL JOURNAL OF ENERGY RESEARCH*, 2006.
- [15] S. H. Moon, G. Hwang, S. C. Ko, and Y. T. Kim, "Experimental study on the thermal performance of micro-heat pipe with cross-section of polygon," *Microelectronics Reliability*, vol. 44, pp. 315-321, 2004.
- [16] C. C. Silverstein, *Design and Technology of Heat pipes for cooling and Heat exchange*: CRC; 1 edition (August 1, 1992), 1992.
- [17] S. Dharmalingam and K. K. Tio, "The effect of type of working fluid on the heat transport capacity of a micro heat pipe," presented at 3rd International Conference on Microchannels and Minichannels, ICMM2005, Jun 13-15 2005, Toronto, ON, Canada, 2005.
- [18] D. Sugumar and K. K. Tio, "Heat transport limitation of a triangular micro heat pipe," presented at First International Conference on Microchannels and Minichannels, Apr 24-25 2003, Rochester, NY, United States, 2003.
- [19] K.-K. Tio, C. Y. Liu, and K. C. Toh, "Thermal analysis of micro heat pipes using a porous-medium model," *Heat and Mass Transfer/Waerme- und Stoffuebertragung*, vol. 36, pp. 21-28, 2000.
- [20] M. L. B. Guillaume Pandraud, Panagiota Morfouli, Monique Lallemand,, "Influence of the Fluid on the Experimental Performances of Triangular Silicon

- Microheat Pipes," Journal of Electronic Packaging, Transactions of the ASME, vol. Volume 128, pp. 294-296, 2006.
- [21] D. Sugumar and K.-K. Tio, "Thermal analysis of inclined micro heat pipes," Journal of Heat Transfer, vol. 128, pp. 198-202, 2006.
- [22] B. Suman and N. Hoda, "Effect of variations in thermophysical properties and design parameters on the performance of a V-shaped micro grooved heat pipe," International Journal of Heat and Mass Transfer, vol. 48, pp. 2090-2101, 2005.
- [23] G. P. Peterson and H. B. Ma, "Theoretical analysis of the maximum heat transport in triangular grooves: a study of idealized micro heat pipes," presented at Proceedings of the 1995 ASME International Mechanical Engineering Congress and Exposition. Part 1 (of 2), Nov 12-17 1995, San Francisco, CA, USA, 1995.
- [24] B. Suman, "On the fill charge and the sensitivity analysis of a V-shaped micro heat pipe," AIChE Journal, vol. 52, pp. 3041-3054, 2006.
- [25] Y. Cao, A. Faghri, and E. T. Mahefkey, "Micro/miniature heat pipes and operating limitations," presented at 29th National Heat Transfer Conference, Aug 8-11 1993, Atlanta, GA, USA, 1993.
- [26] S. Kalahasti and Y. K. Joshi, "Performance characterization of a novel flat plate micro heat pipe spreader," IEEE Transactions on Components and Packaging Technologies, vol. 25, pp. 554-560, 2002.
- [27] C.-I. Tien, S. Kotake, and N. D. Gakkai, Molecular and Microscale Heat Transfer: Begell House Publishers, Inc., 1994.
- [28] O. S. Nadgauda, "Fabrication, Filling, Sealing and Testing of Micro Heat Pipes," in Mechanical Engineering. Auburn: Auburn University, 2006, pp. 99.

- [29] R. C. Jaeger, Introduction to microelectronic fabrication, vol. 5, Second ed: Prentice Hall, 2001.
- [30] D. K. Harris, O. Nadgauda, Nicole Sanders, C. Ellis, and M. Palmer, "A packaging Sealing Technique for Mercury Filled Microfluidic Devices," presented at IMAPS, Scottsdale, Arizona, USA, 2006.
- [31] S. Launay, V. Sartre, and M. Lallemand, "Experimental study on silicon micro-heat pipe arrays," Applied Thermal Engineering, vol. 24, pp. 233-243, 2004.
- [32] R. W. P. C. Y. HO, P. E. Liley, Journal of Physical and Chemical Reference Data, vol. 3, Supplement No. 1: American Chemical Society and American Institute of Physics for the National Bureau of Standards, 1974.
- [33] J. R. Taylor, An Introduction to Error Analysis: The Study of Uncertainties in Physical Measurements, Second Edition ed: University Science Books, 55D Gate Five Road, Sausalito, CA--94965., 1997.
- [34] P. Ramadas, H. T. Henderson, and G. Badran, "Liquid-metal micro heat pipes incorporated in waste-heat radiator panels," 10th Anniversary Symposium on Space Nuclear Power and Propulsion, pp. 551-557, 1993.
- [35] J. C. Mankins, "Technology Readiness Levels," Advanced Concepts Office, Office of Space Access and Technology, NASA., A White Paper April 6 1995.